

# Koopman Operator Spectrum for Random Dynamical Systems

Nelida Črnjarić-Žić\*, Senka Maćešić† and Igor Mezić‡

June 1, 2022

## Abstract

In this paper we propose a generalized Koopman operator framework for discrete and continuous time random dynamical systems. For the particular classes of random dynamical systems, we provide the results that characterize the spectrum and the eigenfunctions of the stochastic Koopman operator. We discuss the relationship between the spectral properties of the generator of the evolution and the Koopman operator family. The numerical approximations of the spectral objects (eigenvalues, eigenfunctions) of the stochastic Koopman operator are computed by using the state of the art DMD RRR algorithm. We explore its behavior in the stochastic case on several test examples. Moreover, the DMD RRR algorithm is applied in combination with the Hankel matrix and a convergence theorem for Hankel DMD RRR in the stochastic case is proved.

*Keywords:* stochastic Koopman operator, random dynamical systems, stochastic differential equations, dynamic mode decomposition

*Mathematics Subject Classification:* 37H10, 47B33, 37M99, 65P99

## 1 Introduction

Prediction and control of the evolution of large complex dynamical systems is a modern-day science and engineering challenge. Some dynamical systems can be modeled well enough by using the standard mathematical tools, such as, for example, differential or integral calculus. In these cases the simplifications of the system are typically introduced neglecting some of the phenomena with small impact on the behavior of the system. However, there are many dynamical systems for which the mathematical model is too complex or even does not exist, but data can be obtained by monitoring some observables of the considered system. In this context, data-driven analysis methods need to be developed, including techniques to extract simpler, representative components of the process that can be used for modeling and prediction.

---

\*Faculty of Engineering, University of Rijeka, Croatia, nelida@riteh.hr

†Faculty of Engineering, University of Rijeka, Croatia, senka.macesic@riteh.hr

‡Faculty of Mechanical Engineering and Mathematics, University of California, Santa Barbara, CA, 93106, USA mezić@engr.ucsb.edu

One possible approach for decomposing the complex systems into simpler structures is via the spectral decomposition of the Koopman operator related to the considered dynamical system. Koopman operator was introduced in [12] in the measure-preserving setting, as a composition operator acting on the Hilbert space of observable functions. The increased interest in the spectral operator-theoretic approach to dynamical systems in last decade starts with the works [21] and [17], where the problem of decomposing the evolution of an ergodic dissipative dynamical system from the perspective of operator theory was studied. The application of the theory to complex systems are numerous, for example in turbulent fluid flows [3, 28], infectious disease dynamics [22], power systems [31, 33] etc. The advantage of using the Koopman operator framework lies in the fact that it can be applied within the data-driven environment, even if the underlying mathematical model is not known. In addition to analysis of the system properties the Koopman decomposition of complex dynamical structures can provide approximations to the evolution of a possibly high dimensional system in lower dimensions, enabling model reduction. An overview of the spectral properties of the Koopman operator and its applications is given in [18, 4].

A variety of methods for determining the numerical approximation of the Koopman spectral decomposition, known under the name Koopman Mode Decomposition (KMD) has been developed. KMD consist of the Koopman eigenvalues, eigenfunctions and modes, which are the building blocks of the evolutions of observables under the dynamics of a complex dynamical system. A general method for computing the Koopman modes, based on the rigorous theoretical results for the generalized Laplace transform, is known under the name Generalized Laplace Analysis (GLA) [18, 4]. Another method is the Dynamic Mode Decomposition (DMD) method. DMD was firstly introduced in [25] for the study of the fluid flows, without any reference to the Koopman operator. The connection between the KMD and DMD was first pointed out in [24]. Like GLA, DMD is a data driven technique. Due to the fact it could be numerically implemented relatively easily since it relies on standard linear algebra concepts, this method become extremely popular in the data-driven systems research community. Starting with [26] many versions of the DMD algorithm have been introduced to efficiently compute the spectral objects of the Koopman operator under various assumptions on the data. In [36] the exact DMD algorithm was introduced, while in [37] the extension of the DMD algorithm, under the name Extended Dynamic Mode Decomposition (EDMD) was proposed. These two methods rely on the more standard approaches to exhibiting a linear operator on a basis, rather than a sampling method as in companion DMD. Susuki and Mezić introduced in [32] a further extension of the DMD algorithm, which combines the Prony method with the DMD algorithm, so that the Hankel matrix is used instead of the companion matrix to compute the Koopman spectrum on the single observable as well as on the vector of observable functions. In [1], Arbabi and Mezić referred to this algorithm as to the Hankel DMD and proved that under certain assumptions the obtained eigenvalues and eigenvectors converge to the exact eigenvalues and eigenvectors of the Koopman operator. The assumptions were removed, and further connections between the spectra of EDMD matrices and eigenvalues of the Koopman operator were proven in [13].

The majority of works analyzing or practically using the spectral properties of the Koopman operator assume that the dynamical system under consideration is autonomous. Similarly, the proposed numerical algorithms for evaluating KMD were almost exclusively applied to autonomous dynamical systems. Generalization of the Koopman operator

framework to nonautonomous system was introduced in [20], where the definition of nonautonomous Koopman eigenvalues, eigenfunction and modes, as building blocks of the dynamical system, is given. KMD for nonautonomous systems was studied in [16], where the possibility of using the Arnoldi-like DMD algorithms for evaluating the Koopman eigenvalues and eigenvectors in the nonautonomous case was carefully explored and the appropriate extensions of the algorithm were proposed. The extension of DMD to nonautonomous systems was done in [14], where the system including multiple time scales were considered and the multiresolution DMD algorithm was successfully applied to the non-stationary data.

Another possible generalization of the Koopman operator framework is its extension to random dynamical systems (RDS) and stochastic systems. In this paper we make the distinction between these two classes of probabilistic systems, where stochastic systems have nowhere differentiable sample paths, and RDS sample paths have some regularity properties [2, 30]. The Koopman operator for discrete RDS was firstly introduced in [21, 17], where the action of the associated Koopman operator on an observable was defined by taking an expectation of values of the observable at the next time step. In this work we extend this definition to continuous-time RDS and stochastic systems, and provide a definition of the associated eigenvalues and eigenfunctions. We explore some properties of the associated random and stochastic Koopman operator family. For the systems defined by autonomous stochastic differential equation, we derive the generator of the associated stochastic Koopman operator family and discuss the relationship between the spectral objects of the generator and of the Koopman operator family members. The characterization of the dynamics of such systems by using the eigenvalues and the eigenfunctions of the related generators is studied in recent papers [29], [35] and [7]. Giannakis in [7] develops a framework for the KMD based on the representation of the Koopman operator in a smooth orthonormal bases determined from the time-ordered noisy data through the diffusion map algorithm. Using this representation, the Koopman eigenfunctions are determined as the eigenfunctions of the related advection-diffusion operator. A similar approach by using the manifold learning technique via diffusion maps was used in [29] to capture the inherent coordinates for building an intrinsic representation of the dynamics driven by the Langevin stochastic differential equation. The linear operator is then used to describe the evolution of the constructed coordinates on the state space of the dynamical system. The obtained coordinates are approximations of the eigenfunctions of the stochastic Koopman generator, so that the described approach is closely connected with the Koopman operator techniques for building the representation of the system dynamics.

In order to numerically approximate the spectral objects of the stochastic Koopman operator, we explore the possibility of application of DMD algorithms that were originally developed for evaluating KMD in deterministic systems. As already mentioned, algorithms that are typically used to extract relevant spectral information are, for example, the Schmid DMD algorithm [26, 27], the exact DMD algorithm [36], and the Arnoldi-like algorithm [24]. The application of DMD algorithm to noisy data is studied, for example, in recent papers [8] and [34]. In order to remove the bias errors produced by using the standard DMD algorithms on data with the observation noise that can arise, for example, as a consequence of imprecise measurements, Hemati et al. developed in [8] the total least squares DMD, which for the described type of data outperforms the standard DMD. Takeishi et al. considered in [34] the numerical approximations of spectral objects

of the stochastic Koopman operator for the RDS with observation noise by using the DMD algorithm. Due to the systematic error produced by the standard DMD algorithm they developed the version of the algorithm that takes into account the observation noise and refer to it as the subspace DMD algorithm. Under the assumption that the data are obtained with the observable spanning a subspace invariant to the Koopman operator and some additional assumptions, they proved that the algorithm gives the eigenvalues converging to the exact eigenvalues of the stochastic Koopman operator. The necessity of using such approach is a consequence of the observation noise, which appears in the data they considered. However, as stated in [5], there exist some numerical issues that can arise in mentioned algorithms leading to poor approximations of eigenvalues and eigenvectors. In order to overcome this difficulties, Drmač et al. proposed in [5] an enhanced data driven algorithm for computing DMD, called DMD refined Rayleigh Ritz algorithm, or shortly DMD RRR algorithm, which has significantly better properties than previous versions of DMD algorithms and therefore we use it in this work. In most considered RDS examples, we first determine the Koopman eigenvalues and eigenfunctions of the related deterministic dynamical system and then explore the algorithm behavior on the considered RDS. Despite the fact that in some cases we noticed high sensitivity of the numerical algorithm to the noise introduced into the system, in most cases very satisfactory approximations are obtained.

The paper is organized as follows. In Section 2, the definition of the Koopman operator family for discrete and continuous-time RDS is given. This section is divided into three subsections. In the first subsection the Koopman operator related to the chosen discrete RDS is studied. In the second subsection we consider the properties of the Koopman operator associated to the RDS corresponding to the random differential equations. These RDS are obtained by solving random differential equations pathwise and are absolutely continuous with respect to time. On the other hand, there is a large class of continuous-time stochastic systems, which are not absolutely continuous and locally not of bounded variation, but yet have generators. We study the properties of the Koopman operator associated to such systems, driven by the stochastic differential equations, in the third subsection. We provide the results regarding the spectral objects of the stochastic Koopman operator and derive its eigenvalues and eigenfunctions for some examples. In Section 3, a brief description of the DMD RRR algorithm is provided and its application to RDS is described. We prove that for the ergodic systems, the eigenvalues and eigenvectors obtained by applying the DMD RRR algorithm to the Hankel matrix converge to the true eigenvalues and eigenvectors of the stochastic Koopman operator. A similar convergence is proved in [34], under the assumption that the noise is modeled by the independent identically distributed random variables. Here we provide a proof for a more general RDS and use different approach based on the fact that the matrix representation of the finite dimensional approximation of the Koopman operator in the Krylov basis is equal to the companion matrix. Finally, the computations of Koopman eigenvalues and eigenfunctions by using the described algorithm are illustrated in several numerical examples in Section 4.

## 2 Stochastic Koopman operator

First, we give the definition and a brief description of RDS, which follows terminology and results in [2].

Let  $(\Omega, \mathcal{F}, P)$  be a probability space and  $\mathbb{T}$  a semigroup (we can think of it as time). Suppose that  $(\theta(t))_{t \in \mathbb{T}}$  is measure-preserving dynamical system on a probability space  $(\Omega, \mathcal{F}, P)$  for which  $\theta(t)$  is homomorphism of  $(\Omega, \mathcal{F}, P)$  to itself with the property  $\theta(t)P = P$ , i.e.  $P$  is invariant with respect to each  $\theta(t)$ . The quadruple  $(\Omega, \mathcal{F}, P, (\theta(t))_{t \in \mathbb{T}})$  is then a driving dynamical system.

A random dynamical system (RDS) on the manifold  $(M, \mathcal{S})$  over a dynamical system  $(\Omega, \mathcal{F}, P, (\theta(t))_{t \in \mathbb{T}})$  is the measurable mapping  $\varphi : \mathbb{T} \times \Omega \times M \rightarrow M$  satisfying a cocycle property with respect to  $\theta(\cdot)$ , which means that the mappings  $\varphi(t, \omega) := \varphi(t, \omega, \cdot) : M \rightarrow M$  form the cocycle over  $\theta(\cdot)$ , i.e.:

$$\varphi(0, \omega) = id_M, \quad \varphi(t + s, \omega) = \varphi(t, \theta(s)\omega) \circ \varphi(s, \omega), \quad \text{for all } s, t \in \mathbb{T}, \omega \in \Omega. \quad (1)$$

In what follows we describe the canonical realization of a stochastic process and give the example of a dynamical system  $(\theta(t))_{t \in \mathbb{T}}$  on a probability space generated by the given stochastic process.

Let  $\tilde{\Omega}$  be a probability space endowed with a probability measure, and  $(B, \mathcal{B})$  a measurable state space. For a semigroup  $\mathbb{T}$ , let  $\tilde{\xi} = (\tilde{\xi}_t)_{t \in \mathbb{T}}$  be a stochastic process on  $\tilde{\Omega}$ , i.e., a family of random variables  $\tilde{\xi}_t : \tilde{\Omega} \rightarrow B$ ,  $t \in \mathbb{T}$ . This family generates a probability measure  $P$  on  $B^{\mathbb{T}}$ , which is a joint probability measure of the stochastic process, so the stochastic process  $\tilde{\xi}$  can be also seen as a random variable  $\tilde{\xi} : \tilde{\Omega} \rightarrow B^{\mathbb{T}}$ . The coordinate functions  $\xi_t(\omega) = \omega(t)$  on  $(B^{\mathbb{T}}, \mathcal{B}^{\mathbb{T}}, P)$  define another stochastic process  $\xi$ . Since the stochastic processes  $\tilde{\xi}$  and  $\xi$  generate the same probability measure on  $B^{\mathbb{T}}$ , they are equivalent and  $\xi$  is called the canonical realization of  $\tilde{\xi}$  on  $(\Omega, \mathcal{F}, P) = (B^{\mathbb{T}}, \mathcal{B}^{\mathbb{T}}, P)$ .

The canonical realization can also be viewed as the composition of the shift transformation  $\theta(t) : B^{\mathbb{T}} \rightarrow B^{\mathbb{T}}$  and of the canonical projection  $\pi : B^{\mathbb{T}} \rightarrow B$  defined by

$$\theta(t)\omega(\cdot) := \omega(t + \cdot), \quad t \in \mathbb{T}, \quad (2)$$

and

$$\pi(\omega(\cdot)) = \omega(0), \quad (3)$$

respectively. If  $(B, \mathcal{B})$  is the topological space with its Borel  $\sigma$ -algebra, then the group of the shift transformations  $(\theta(t))_{t \in \mathbb{T}}$  defined with (2) is the dynamical system on  $(\Omega, \mathcal{F}, P) = (B^{\mathbb{T}}, \mathcal{B}^{\mathbb{T}}, P)$  (see [2]).

In the next definition we introduce the Koopman operator family associated to the RDS.

**Definition 1.** *The stochastic Koopman operator  $\mathcal{K}^{S,t}$  associated to the RDS  $\varphi$  is defined on a space of scalar valued functions  $f : M \rightarrow \mathbb{C}$  (observables) by*

$$\mathcal{K}^{S,t}f(\mathbf{x}) = \mathbb{E}_{\Omega}[f(\varphi(t, \omega)\mathbf{x})], \quad \mathbf{x} \in M. \quad (4)$$

*We refer to the family of operators  $\mathcal{K}^{S,t}$ , parametrized by time  $t$ , the stochastic Koopman operator family.*

**Proposition 1.** *The stochastic Koopman operator family satisfies the semigroup property, i.e.  $\mathcal{K}^{S,t+s} = \mathcal{K}^{S,s} \circ \mathcal{K}^{S,t}$ .*

*Proof.* Observe that

$$\mathcal{K}^{S,0} f(\mathbf{x}) = \mathbb{E}_\Omega[f(\varphi(0, \omega)\mathbf{x})] = \mathbb{E}_\Omega[f(\mathbf{x})] = f(\mathbf{x}), \quad (5)$$

where the second equality follows from (1), i.e.  $\mathcal{K}^{S,0} = id$  on the set of all observables. Further, we have

$$\begin{aligned} \mathcal{K}^{S,t+s} f(\mathbf{x}) &= \mathbb{E}_\Omega[f(\varphi(t+s, \omega)\mathbf{x})] = \int_\Omega f(\varphi(s+t, \omega)\mathbf{x}) dP(\omega) \\ &= \int_\Omega \left( \int_\Omega f(\varphi(t, \omega_1) \circ \varphi(s, \omega)\mathbf{x}) dP(\omega_1) \right) dP(\omega) \\ &= \int_\Omega (\mathcal{K}^{S,t} f)(\varphi(s, \omega)\mathbf{x}) dP(\omega) = \mathcal{K}^{S,s} (\mathcal{K}^{S,t} f(\mathbf{x})), \end{aligned} \quad (6)$$

where the third equality follows from the invariance of  $P$  under  $\theta$ .  $\square$

In what follows we will consider the RDS on a probability space  $(\Omega, \mathcal{F}, P) = (B^\mathbb{T}, \mathcal{B}^\mathbb{T}, P)$ , where the joint probability measure  $P$  is generated by a stochastic process  $\xi$  and the homomorphism  $\theta(t)$  is the shift transformation defined by (2).

## 2.1 Koopman operator on the discrete RDS

For a discrete time RDS we have  $\mathbb{T} = \mathbb{Z}^+ \cup \{0\}$ . Denote the one-step shift transformation with  $\psi = \theta(1)$ , where  $\theta$  is defined by (2). The discrete RDS  $\varphi(n, \omega)$  can be defined by the one step map  $T(\omega, \cdot) : M \rightarrow M$

$$T(\omega, \cdot) := \varphi(1, \omega),$$

since by applying the cocycle property one gets

$$\varphi(n, \omega) = T(\psi^{n-1}(\omega), \cdot) \circ \cdots \circ T(\psi(\omega), \cdot) \circ T(\omega, \cdot), \quad n \geq 1. \quad (7)$$

According to (1),  $\varphi(0, \omega) = id_M$ . The action of the discrete RDS  $\varphi(n, \omega)$  on  $\mathbf{x} \in M$  gives its value at  $n$ -th step and we denote it as

$$T^n(\omega, \mathbf{x}) = \varphi(n, \omega)\mathbf{x}. \quad (8)$$

The discrete RDS can be considered as the solution of the random difference equation

$$\mathbf{x}_{n+1} = T(\psi^n(\omega), \mathbf{x}_n), \quad n \geq 0, \quad \mathbf{x}_0 = \mathbf{x}. \quad (9)$$

The stochastic Koopman operator family  $\mathcal{K}^{S,n}$ ,  $n \geq 0$  associated to discrete RDS is defined by (4). Since the one step map  $T(\omega, \cdot)$  is the generator of the discrete RDS, it is enough to consider the generator of the stochastic Koopman operator family

$$\mathcal{K}^S f(\mathbf{x}) = \mathcal{K}^{S,1} f(\mathbf{x}) = \mathbb{E}_\Omega[f(T(\omega, \mathbf{x}))]. \quad (10)$$

**Remark 1.** *It is common to use the term stochastic Koopman operator for the operator  $\mathcal{K}^S$  in (10). However we will refer to it as to the generator of the stochastic Koopman operator family, or shortly, the stochastic Koopman generator, to be consistent with the terminology used in the continuous-time case.*

The eigenvalues  $\lambda_j^S$  and the eigenfunctions  $\phi_j$  of the operator  $\mathcal{K}^S$  are defined by

$$\mathcal{K}^S \phi_j(\mathbf{x}) = \lambda_j^S \phi_j(\mathbf{x}). \quad (11)$$

**Example 1** (Noisy rotation on the circle). *We describe here the example considered in [11]. A deterministic dynamical system representing the rotation  $T$  on the unit circle  $S^1$  is defined by*

$$T(x) = x + \theta, \quad (12)$$

where  $\theta \in S^1$  is constant number. We consider here its stochastic perturbation, i.e. a discrete RDS defined by (9) with the one step map  $T : \Omega \times S^1 \rightarrow S^1$ :

$$T(\omega, x) = x + \theta + \pi(\omega), \quad (13)$$

where  $\omega \in [-\delta/2, \delta/2]^{\mathbb{Z}}$  and  $\pi(\cdot)$  is the canonical projection defined by (3). The coordinates  $\omega_i$  are induced by independent identically distributed random variables  $\xi_i$  ( $\xi_i(\omega) = \omega_i$ ), which have the uniform distribution on the interval  $[-\delta/2, \delta/2]$  for some  $\delta > 0$ . According to (10), the action of the associated stochastic Koopman generator on an observable function  $f : S^1 \rightarrow \mathbb{C}$  is given by

$$\mathcal{K}^S f(x) = \mathbb{E}_{\Omega}[f(T(\omega, x))] = \frac{1}{\delta} \int_{-\delta/2}^{\delta/2} f(x + \theta + \omega_0) d\omega_0. \quad (14)$$

For the functions

$$\phi_n(x) = \exp(i2\pi nx), \quad n = 1, 2, \dots \quad (15)$$

the following equality holds

$$\begin{aligned} \mathcal{K}^S \phi_n(x) &= \frac{1}{\delta} \int_{-\delta/2}^{\delta/2} \exp(i2\pi n(x + \theta + \omega_0)) d\omega_0 \\ &= \frac{\sin(n\pi\delta)}{n\pi\delta} \exp(i2\pi n\theta) \exp(i2\pi nx) \\ &= \frac{\sin(n\pi\delta)}{n\pi\delta} \exp(i2\pi n\theta) \phi_n(x). \end{aligned} \quad (16)$$

We easily conclude that (15) are the eigenfunctions of the stochastic Koopman generator with corresponding eigenvalues

$$\lambda_n^S = \frac{\sin(n\pi\delta)}{n\pi\delta} \exp(i2\pi n\theta), \quad n = 1, 2, \dots \quad (17)$$

It is known that the eigenvalues of the Koopman generator related to deterministic dynamical system (12) lie on the unit circle and are equal to  $\lambda_n = \exp(i2\pi n\theta)$ , while the eigenfunctions are the same as for the considered discrete RDS. Moreover, it is interesting to observe that for rational  $\theta$  the eigenspaces are in deterministic case, i.e. for  $\delta = 0$ , infinite dimensional, while they are one dimensional in the stochastic case when  $\delta > 0$ .

In the proposition that follows we consider the properties of the Koopman operator related to the discrete RDS induced by a linear map  $T$ .

**Proposition 2.** *Let  $T : \Omega \times \mathbb{R}^d \rightarrow \mathbb{R}^d$  be a linear discrete RDS defined by*

$$T(\omega, \mathbf{x}) = \mathbf{A}(\omega)\mathbf{x}, \quad (18)$$

where  $\mathbf{A} : \Omega \rightarrow \mathbb{R}^{d \times d}$  is measurable. Assume that  $\hat{\mathbf{A}} = \mathbb{E}_\Omega[\mathbf{A}(\omega)]$  is diagonalizable, with simple eigenvalues  $\hat{\lambda}_j$  and left eigenvectors  $\hat{\mathbf{w}}_j$ ,  $j = 1, \dots, d$ . Then the eigenfunctions of the stochastic Koopman generator  $\mathcal{K}^S$  are

$$\phi_j(\mathbf{x}) = \langle \mathbf{x}, \hat{\mathbf{w}}_j \rangle, \quad j = 1, \dots, d, \quad (19)$$

with the corresponding eigenvalues  $\lambda_j^S = \hat{\lambda}_j$ .

Moreover, if matrices  $\mathbf{A}(\omega)$ ,  $\omega \in \Omega$  commute and are diagonalizable with the simple eigenvalues  $\lambda_j(\omega)$  and corresponding left eigenvectors  $\mathbf{w}_j$ ,  $j = 1, \dots, d$ , then

$$\hat{\mathbf{w}}_j = \mathbf{w}_j \quad \text{and} \quad \hat{\lambda}_j = \mathbb{E}_\Omega[\lambda_j(\omega)].$$

*Proof.* The action of the stochastic Koopman generator on functions defined with (19) is equal to

$$\begin{aligned} \mathcal{K}^S \phi_j(\mathbf{x}) &= \mathbb{E}_\Omega[\langle \mathbf{A}(\omega)\mathbf{x}, \hat{\mathbf{w}}_j \rangle] = \mathbb{E}_\Omega[\langle \mathbf{x}, \mathbf{A}^*(\omega)\hat{\mathbf{w}}_j \rangle] = \langle \mathbf{x}, \mathbb{E}_\Omega[\mathbf{A}^*(\omega)]\hat{\mathbf{w}}_j \rangle \\ &= \langle \mathbf{x}, \hat{\mathbf{A}}^*\hat{\mathbf{w}}_j \rangle = \hat{\lambda}_j \langle \mathbf{x}, \hat{\mathbf{w}}_j \rangle = \hat{\lambda}_j \phi_j(\mathbf{x}), \end{aligned} \quad (20)$$

where we have used that

$$\mathbb{E}_\Omega[\mathbf{A}^*(\omega)] = (\mathbb{E}_\Omega[\mathbf{A}(\omega)])^* = \hat{\mathbf{A}}^*.$$

In the case when matrices  $\mathbf{A}(\omega)$  commute and are diagonalizable, they have the same set of left and right eigenvectors  $(\mathbf{w}_j, \mathbf{v}_j)$ ,  $j = 1, \dots, d$ , which can be normalized so that  $\langle \mathbf{w}_i, \mathbf{v}_j \rangle = \delta_{ij}$  ( $\delta_{ij}$  is Kronecker delta symbol). If  $\mathbf{W}$  and  $\mathbf{V}$  are matrices of left and right eigenvectors respectively, and  $\mathbf{\Lambda}(\omega) = \text{diag}(\lambda_1(\omega), \dots, \lambda_d(\omega))$ , then  $\mathbf{A}(\omega) = \mathbf{V}\mathbf{\Lambda}(\omega)\mathbf{W}^*$  and

$$\hat{\mathbf{A}} = \mathbb{E}_\Omega[\mathbf{A}(\omega)] = \mathbf{V}\mathbb{E}_\Omega[\mathbf{\Lambda}(\omega)]\mathbf{W}^*.$$

Thus,  $\hat{\mathbf{w}}_j = \mathbf{w}_j$  and  $\hat{\lambda}_j = \mathbb{E}_\Omega[\lambda_j(\omega)]$ . □

**Remark 2.** *We will use the term principal eigenfunctions for the eigenfunctions of the form  $\phi_j(\mathbf{x}) = \langle \mathbf{x}, \mathbf{w}_j \rangle$  that appear in Proposition 2 and in some other propositions in the rest of the paper. Also, the eigenvalues corresponding to them we call the principal eigenvalues.*

**Remark 3.** *Consider the case when randomness is additive, i.e. when the one-step map is given by*

$$T(\omega, \mathbf{x}) = \mathbf{A}\mathbf{x} + \theta(t)\omega.$$

Suppose that  $\mathbb{E}_\Omega[\theta(t)\omega] = 0$  for every  $t$  and that the matrix  $\mathbf{A}$  is diagonalizable with simple eigenvalues  $\lambda_j$ ,  $j = 1, \dots, d$ . Then the eigenfunctions of the stochastic Koopman generator  $\mathcal{K}^S$  are principal eigenfunctions of the form  $\phi_j(\mathbf{x}) = \langle \mathbf{x}, \mathbf{w}_j \rangle$ ,  $j = 1, \dots, d$ , where  $\mathbf{w}_j$ ,  $j = 1, \dots, d$  are left eigenvectors of  $\mathbf{A}$ , while its eigenvalues coincide with the eigenvalues of the matrix  $\mathbf{A}$ .



## 2.2 Koopman operator family of the RDS driven by the random differential equations

Suppose that  $\mathbb{T} = \mathbb{R}$ . We consider here a continuous-time RDS driven by the random differential equation (RDE) of the following form

$$\dot{\mathbf{x}} = F(\theta(t)\omega, \mathbf{x}), \quad (21)$$

defined on the manifold  $M$ , where  $\omega \in \Omega = B^{\mathbb{R}}$  is an element in the probability space  $\Omega$  associated with the random dynamics and equipped with the probability measure and  $\theta(t)$  is shift operator defined by (2). This RDE generates an RDS  $\varphi$  over  $\theta$ , which is absolutely continuous with respect to time and whose action is defined by

$$\varphi(t, \omega)\mathbf{x} = \mathbf{x} + \int_0^t F(\theta(s)\omega, \varphi(s, \omega)\mathbf{x})ds. \quad (22)$$

The properties of this RDS under different regularity properties of the function  $F$  can be found in [2]. A set of trajectories starting at  $\mathbf{x}$  that are generated by (21) is given by

$$X(t, \omega, \mathbf{x}) = \varphi(t, \omega)\mathbf{x} \quad (23)$$

and it defines the family of random variables  $X(t, \omega, \mathbf{x}), t \in \mathbb{T}, \omega \in \Omega$ . We say that this is a solution of the RDE with the initial condition  $X(0, \omega, \mathbf{x}) = \mathbf{x}$ . Since the solutions of the RDE are defined pathwise, for each fixed  $\omega$  the trajectory can be determined as a solution of deterministic ordinary differential equation, so that the RDE (21) can be seen as a family of ordinary differential equations. In this type of equations the randomness refers just to the random parameters, which do not depend on the state of the system. Since the solutions of (21) are continuous and of bounded variation, the random part is also of bounded variation.

We will consider here the Koopman operator family  $\mathcal{K}^{S,t}$  defined by (4) that is related to this RDS. Similarly as in discrete case, we will refer to the observables  $\phi^{S,t} : M \rightarrow \mathbb{C}$  that satisfy equation

$$\mathcal{K}^{S,t}\phi^{S,t}(\mathbf{x}) = e^{\lambda^S(t)}\phi^{S,t}(\mathbf{x}) \quad (24)$$

as to the eigenfunctions of the stochastic Koopman operator family. The associated values  $\lambda^S(t)$  are its eigenvalues.

In the next proposition we derive the eigenvalues and the eigenvectors of the stochastic Koopman operators associated to the linear RDS.

**Proposition 3.** *If  $\mathbf{A} : \Omega \rightarrow \mathbb{R}^{d \times d}$  and  $\mathbf{A} \in L^1(\Omega, \mathcal{F}, P)$  then RDE*

$$\dot{\mathbf{x}} = \mathbf{A}(\theta(t)\omega)\mathbf{x}, \quad (25)$$

*generates a linear RDS  $\Phi$  satisfying*

$$\Phi(t, \omega) = \mathbf{I} + \int_0^t \mathbf{A}(\theta(s)\omega)\Phi(s, \omega)ds. \quad (26)$$

*Assume that  $\hat{\Phi}(t) = \mathbb{E}_{\Omega}[\Phi(t, \omega)]$  is diagonalizable, with simple eigenvalues  $\hat{\mu}_j^t = e^{\hat{\lambda}_j(t)}$  and left eigenvectors  $\hat{\mathbf{w}}_j^t, j = 1, \dots, d$ . Then*

$$\phi_j^{S,t}(\mathbf{x}) = \langle \mathbf{x}, \hat{\mathbf{w}}_j^t \rangle, \quad j = 1, \dots, d, \quad (27)$$

are the principal eigenfunctions of the stochastic Koopman operator  $\mathcal{K}^{S,t}$  with corresponding principal eigenvalues  $\lambda_j^S(t) = \hat{\lambda}_j(t)$ ,  $j = 1, \dots, d$ .

Moreover, if matrices  $\mathbf{A}(\omega)$  commute and are diagonalizable with the simple eigenvalues  $\lambda_j(\omega)$  and corresponding left eigenvectors  $\mathbf{w}_j$ ,  $j = 1, \dots, d$ , then

$$\hat{\mathbf{w}}_j^t = \mathbf{w}_j \quad \text{and} \quad e^{\lambda_j^S(t)} = \mathbb{E}_\Omega \left[ e^{\int_0^t \lambda_j(\theta(s)\omega) ds} \right].$$

*Proof.* The first part of the proposition follows from [2], Example 2.2.8.

Furthermore, the action of the stochastic Koopman operator on functions defined by (27) is equal to

$$\begin{aligned} \mathcal{K}^{S,t} \phi_j^{S,t}(\mathbf{x}) &= \mathbb{E}_\Omega[\langle \Phi(t, \omega) \mathbf{x}, \hat{\mathbf{w}}_j^t \rangle] = \mathbb{E}_\Omega[\langle \mathbf{x}, \Phi^*(t, \omega) \hat{\mathbf{w}}_j^t \rangle] = \langle \mathbf{x}, \mathbb{E}_\Omega[\Phi^*(t, \omega)] \hat{\mathbf{w}}_j^t \rangle \\ &= \langle \mathbf{x}, \hat{\Phi}^*(t) \hat{\mathbf{w}}_j^t \rangle = \hat{\mu}_j^t(\mathbf{x}, \hat{\mathbf{w}}_j^t) = e^{\hat{\lambda}_j(t)} \phi_j^{S,t}(\mathbf{x}) \end{aligned} \quad (28)$$

In the case when matrices  $\mathbf{A}(\omega)$  commute and are diagonalizable, they have the same set of left and right eigenvectors  $(\mathbf{w}_j, \mathbf{v}_j)$ ,  $j = 1, \dots, d$ . If  $\mathbf{W}$  and  $\mathbf{V}$  are matrices of left and right eigenvectors respectively, and  $\mathbf{\Lambda}(\omega) = \text{diag}(\lambda_1(\omega), \dots, \lambda_d(\omega))$ , then  $\mathbf{A}(\omega) = \mathbf{V} \mathbf{\Lambda}(\omega) \mathbf{W}^*$  and

$$\Phi(t, \omega) = e^{\int_0^t \mathbf{A}(\theta(s)\omega) ds} = \mathbf{V} e^{\int_0^t \mathbf{\Lambda}(\theta(s)\omega) ds} \mathbf{W}^*.$$

Therefore

$$\hat{\Phi}(t) = \mathbf{V} \mathbb{E}_\Omega \left[ e^{\int_0^t \mathbf{\Lambda}(\theta(s)\omega) ds} \right] \mathbf{W}^*$$

and we easily conclude that  $\hat{\mathbf{w}}_j = \mathbf{w}_j$  and  $e^{\lambda_j^S(t)} = \mathbb{E}_\Omega \left[ e^{\int_0^t \lambda_j(\theta(s)\omega) ds} \right]$ . □

**Example 2** (Linear scalar RDS). Suppose that linear scalar RDE is given by

$$\dot{x} = a(\pi(\theta(t)\omega))x, \quad (29)$$

where  $a : \Omega \rightarrow \mathbb{R}$  is random variable with finite moments and independent of the initial condition  $X(0, \omega)$ ,  $\omega \in \Omega$ . Assume that  $\pi(\theta(t)\omega)$  is a canonical realization of a stationary stochastic process, where projection  $\pi(\cdot)$  is given by (3). It follows that  $a(\pi(\theta(t)\omega))$  are independent identically distributed and with no dependence of time  $t$ , so that the noise introduced in this way is memoryless. If the moment generating function  $\mathcal{M}_{a(\omega)}(t)$  defined by  $\mathcal{M}_a(t) = \mathbb{E}_\Omega[e^{ta(\omega)}]$  is analytic for  $|t| < R$ , then for  $t < R$ , there exists a unique solution of (29), which can be expressed as

$$X(t, \omega, x) = \varphi(t, \omega)x = x e^{\int_0^t a(\pi(\theta(s)\omega)) ds}. \quad (30)$$

for the initial condition  $X(0, \omega, x) = x$  [30]. The action of the stochastic Koopman operator on the full state observable function  $\phi(x) = x$  is then

$$\mathcal{K}^{S,t} x = \mathbb{E}_\Omega[\varphi(t, \omega)x] = \mathbb{E}_\Omega \left[ x e^{\int_0^t a(\pi(\theta(s)\omega)) ds} \right] = \mathbb{E}_\Omega \left[ e^{a(\omega)t} \right] x, \quad (31)$$

where in the last equality we use the fact that all  $a(\pi(\theta(t)\omega))$  are i.i.d. and independent of time  $t$ . Thus,  $\phi(x) = x$  is the eigenfunction of the stochastic Koopman operator and the corresponding eigenvalue satisfies

$$e^{\lambda^S(t)} = \mathbb{E}_\Omega \left[ e^{a(\omega)t} \right] = \mathcal{M}_{a(\omega)}(t).$$

### 2.2.1 Generator of the Koopman operator family

Define the generator of the stochastic Koopman family  $\mathcal{K}^{S,t}$  on the smooth function  $f : M \rightarrow \mathbb{C}$  by the limit

$$\mathcal{K}^S f(\mathbf{x}) = \lim_{t \rightarrow 0+} \frac{\mathcal{K}^{S,t} f(\mathbf{x}) - f(\mathbf{x})}{t}, \quad (32)$$

if it exists. We have

**Proposition 4.** *If the solution of RDE is differentiable with respect to  $t$  and the stochastic Koopman family  $\mathcal{K}^{S,t}$  is a semigroup, then the action of the generator  $\mathcal{K}^S$  of the stochastic Koopman family  $\mathcal{K}^{S,t}$  on the smooth function  $f : M \rightarrow \mathbb{C}$  is*

$$\mathcal{K}^S f(\mathbf{x}) = \mathbb{E}_\Omega [F(\omega, \mathbf{x})] \cdot \nabla f(\mathbf{x}). \quad (33)$$

*Proof.*

$$\begin{aligned} \mathcal{K}^S f(\mathbf{x}) &= \lim_{t \rightarrow 0+} \frac{\mathcal{K}^{S,t} f(\mathbf{x}) - f(\mathbf{x})}{t} = \lim_{t \rightarrow 0+} \frac{\mathbb{E}_\Omega [f(X(t, \omega, \mathbf{x}))] - f(\mathbf{x})}{t} \\ &= \lim_{t \rightarrow 0+} \frac{\mathbb{E}_\Omega [f(X(t, \omega, \mathbf{x})) - f(\mathbf{x})]}{t} = \mathbb{E}_\Omega \left[ \lim_{t \rightarrow 0+} \frac{f(X(t, \omega, \mathbf{x})) - f(X(0, \omega, \mathbf{x}))}{t} \right] \\ &= \mathbb{E}_\Omega \left[ \left. \frac{d}{dt} f(X(t, \omega, \mathbf{x})) \right|_{t=0} \right] = \mathbb{E}_\Omega \left[ \nabla f(\mathbf{x}) \cdot \left. \frac{d}{dt} X(t, \omega, \mathbf{x}) \right|_{t=0} \right] \\ &= \mathbb{E}_\Omega [F(\omega, \mathbf{x})] \cdot \nabla f(\mathbf{x}). \end{aligned} \quad (34)$$

The replacement of the order of limit and expectation in the second line is justified by dominated convergence theorem where differentiability of the solution with respect to time and the smoothness of  $f$  are taken into account.  $\square$

**Corollary 1.** *Suppose that a stochastic Koopman generator  $\mathcal{K}^S$  associated to RDE (21) exists. If  $\phi_1$  and  $\phi_2$  are the eigenfunctions of  $\mathcal{K}^S$  with the associated eigenvalues  $\lambda_1$  and  $\lambda_2$ , then  $\phi_1 \phi_2$  is also an eigenfunction with the associated eigenvalue  $\lambda_1 + \lambda_2$ .*

*Proof.* Since  $\mathcal{K}^S \phi_i(\mathbf{x}) = \lambda_i \phi_i(\mathbf{x}) = \mathbb{E}_\Omega [F(\omega, \mathbf{x})] \cdot \nabla \phi_i(\mathbf{x})$ , for  $i = 1, 2$ , we have

$$\begin{aligned} \mathcal{K}^S(\phi_1 \phi_2)(\mathbf{x}) &= \mathbb{E}_\Omega [F(\omega, \mathbf{x})] \cdot \nabla(\phi_1 \phi_2)(\mathbf{x}) \\ &= \mathbb{E}_\Omega [F(\omega, \mathbf{x})] \cdot \nabla \phi_1(\mathbf{x}) \cdot \phi_2(\mathbf{x}) + \mathbb{E}_\Omega [F(\omega, \mathbf{x})] \cdot \nabla \phi_2(\mathbf{x}) \cdot \phi_1(\mathbf{x}) \\ &= \lambda_1 \phi_1(\mathbf{x}) \phi_2(\mathbf{x}) + \lambda_2 \phi_2(\mathbf{x}) \phi_1(\mathbf{x}) = (\lambda_1 + \lambda_2)(\phi_1 \phi_2)(\mathbf{x}) \end{aligned}$$

$\square$

**Corollary 2.** *Let  $\phi$  be an eigenfunction associated with eigenvalue  $\lambda$  of the stochastic Koopman generator associated with an RDE (21). Then*

$$\dot{\phi} = \lambda \phi + \tilde{F}(\omega, \mathbf{x}) \cdot \nabla \phi, \quad (35)$$

where

$$\tilde{F}(\omega, \mathbf{x}) = F(\omega, \mathbf{x}) - \mathbb{E}_\Omega [F(\omega, \mathbf{x})].$$

**Remark 4.** Note that in the case when randomness is additive, i.e. when (21) is given by

$$\dot{\mathbf{x}} = G(\mathbf{x}) + \mathbf{B}\theta(t)\omega,$$

the equation

$$\dot{\phi} = \lambda\phi + \mathbf{B}\theta(t)\omega \cdot \nabla\phi, \quad (36)$$

only holds provided  $\mathbb{E}_\Omega[\theta(t)\omega] = 0$  for every  $t$  (the measure on  $\Omega$  is the product measure, thus if this holds for a single  $t$ , it holds for all, and it can be replaced by  $\mathbb{E}_\Omega[\omega] = 0$ ).

**Corollary 3.** Suppose that a stochastic Koopman generator  $\mathcal{K}^S$  associated to linear RDE (25) exists. Also, assume that  $\hat{\mathbf{A}} = \mathbb{E}_\Omega[\mathbf{A}(\omega)]$  is diagonalizable, with simple eigenvalues  $\hat{\lambda}_j$  and left eigenvectors  $\hat{\mathbf{w}}_j$ ,  $j = 1, \dots, d$ . Then

$$\phi_j(\mathbf{x}) = \langle \mathbf{x}, \hat{\mathbf{w}}_j \rangle, \quad j = 1, \dots, d, \quad (37)$$

are the principal eigenfunctions of the operator  $\mathcal{K}^S$ , while  $\lambda_j^S = \hat{\lambda}_j$  are the associated principal eigenvalues.

*Proof.* According to (34), the action of the generator  $\mathcal{K}^S$  of the Koopman operator family associated to RDS driven by linear RDE (25) on a differentiable function  $f : \mathbb{R}^d \rightarrow \mathbb{C}$  is equal to

$$\mathcal{K}^S f(\mathbf{x}) = \mathbb{E}_\Omega[\mathbf{A}(\omega)\mathbf{x}] \cdot \nabla f(\mathbf{x}) = \hat{\mathbf{A}}\mathbf{x} \cdot \nabla f(\mathbf{x}). \quad (38)$$

Thus

$$\mathcal{K}^S \phi_j(\mathbf{x}) = \langle \hat{\mathbf{A}}\mathbf{x}, \mathbf{w}_j \rangle = \langle \mathbf{x}, \hat{\mathbf{A}}^* \mathbf{w}_j \rangle = \hat{\lambda}_j \phi_j(\mathbf{x}),$$

which proves the statement.  $\square$

Provided that the assumptions of Proposition 3 are valid, the principal eigenfunctions  $\phi_j(\mathbf{x})$  given by (37) are the eigenfunctions of each Koopman operator  $\mathcal{K}^{S,t}$  with the corresponding principal eigenvalues  $\lambda_j^{(S)}(t) = \hat{\lambda}_j t$ .

Then, according to Proposition 1, over the space of real analytic functions, the eigenvalues and eigenfunctions of the Koopman operators are of the form

$$\phi(\mathbf{x}) = \phi_1^{n_1}(\mathbf{x}) \cdots \phi_d^{n_d}(\mathbf{x}), \quad \lambda = \sum_{j=1}^d n_j \hat{\lambda}_j,$$

where  $n_j, j = 1, \dots, d$  are non-negative integers. Thus, like in deterministic case, any analytic observable function  $f$  can be represented as linear combination of powers of the principal eigenfunctions [19] and its evolution under the RDS can be obtained using spectral expansion formula.

## 2.3 Koopman operator family of the RDS driven by the stochastic differential equations

Let  $\mathbb{T} = \mathbb{R}^+$ ,  $M = \mathbb{R}^d$  and  $T \in \mathbb{T}$ . Suppose that the stochastic process  $X_t(\omega)$ ,  $t \in [0, T]$ ,  $\omega \in \Omega$  is obtained as a solution of the non-autonomous stochastic differential equation (SDE)

$$dX_t = G(t, X_t)dt + \sigma(t, X_t)dW_t, \quad (39)$$

where  $G : [0, T] \times M \rightarrow M$  and  $\sigma : [0, T] \times M \rightarrow \mathbb{R}^{d \times r}$  are  $L^2$  measurable. Here  $W_t = (W_t^1, \dots, W_t^r)$  denotes the  $r$ -dimensional Wiener process with independent components and standard properties, i.e.  $\mathbb{E}_\Omega(W_t^i) = 0$ ,  $i = 1, \dots, r$ ,  $\mathbb{E}_\Omega(W_t^i W_s^j) = \min\{t, s\} \delta_{ij}$ ,  $i, j = 1, \dots, r$  ( $\delta_{ij}$  is the Kronecker delta symbol). The solution  $X_t(\omega)$  of (39) with the initial condition  $X_{t_0}(\omega)$  is formally defined in terms of Itô integral as

$$X_t(\omega) = X_{t_0}(\omega) + \int_{t_0}^t G(s, X_s(\omega)) ds + \int_{t_0}^t \sigma(s, X_s(\omega)) dW_s. \quad (40)$$

In this non-autonomous setting the SDE generates two parameter family of RDS  $\varphi(t, t_0, \omega)$  such that

$$X_t(\omega) = \varphi(t, t_0, \omega) X_{t_0}(\omega).$$

The generated family of RDS satisfies cocycle property. In contrast to the solutions of RDE, which are absolutely continuous with respect to time, the solutions of SDE are not necessarily absolutely continuous, they can even be nowhere differentiable and locally not of bounded variation with respect to  $t$ . Unlike in RDE where the integral in (22) are for the chosen  $\omega$  defined pathwise, the integrals in (40) are defined only as a limits in probability sense and not as  $\omega$ -wise limits.

The Koopman operator family  $\mathcal{K}^{S, t, t_0}$  related to this RDS is defined by

$$\mathcal{K}^{S, t, t_0} f(\mathbf{x}) = \mathbb{E}_\Omega[f(\varphi(t, t_0, \omega) \mathbf{x})]. \quad (41)$$

In this more general setting with the two-parameter family of Koopman operators (41), the eigenfunctions  $\phi^{S, t, t_0} : M \rightarrow \mathbb{C}$  and eigenvalues  $\lambda^S(t, t_0)$  of the Koopman operator  $\mathcal{K}^{S, t, t_0}$  defined on a finite-time interval satisfy

$$\mathcal{K}^{S, t, t_0} \phi^{S, t, t_0}(\mathbf{x}) = e^{\lambda^S(t, t_0)} \phi^{S, t, t_0}(\mathbf{x}). \quad (42)$$

The following two propositions treat two classes of linear SDE. In the first case we consider the equation in which the stochastic part models the additive noise, while in the second case the stochastic part models the multiplicative noise.

**Proposition 5.** *Let the linear SDE with additive noise be defined by*

$$dX_t = \mathbf{A}(t) X_t dt + \sum_{i=1}^r b^i(t) dW_t^i, \quad (43)$$

where  $\mathbf{A}(t)$  is  $d \times d$  matrix of functions and  $b^i(t)$ ,  $i = 1, \dots, m$  are  $d$ -dimensional vector functions. Assume that the fundamental matrix  $\Phi(t, t_0)$  satisfying the matrix differential equation

$$\dot{\Phi} = \mathbf{A}(t) \Phi, \quad \Phi(t_0) = \mathbf{I} \quad (44)$$

is diagonalizable, with simple eigenvalues  $\mu_j^{t, t_0} = e^{\hat{\lambda}_j(t, t_0)}$  and left eigenvectors  $\hat{\mathbf{w}}_j^{t, t_0}$ ,  $j = 1, \dots, d$ . Then

$$\phi_j^{S, t, t_0}(\mathbf{x}) = \langle \mathbf{x}, \hat{\mathbf{w}}_j^{t, t_0} \rangle, \quad j = 1, \dots, d, \quad (45)$$

are the eigenfunctions of the stochastic Koopman operator  $\mathcal{K}^{S, t, t_0}$ , with corresponding eigenvalues

$$\lambda_j^S(t, t_0) = \hat{\lambda}_j(t, t_0).$$

If matrices  $\mathbf{A}(t)$  commute and are diagonalizable with the simple eigenvalues  $\lambda_j(t)$  and corresponding left eigenvectors  $\mathbf{w}_j$ ,  $j = 1, \dots, d$ , then

$$\hat{\mathbf{w}}_j^{t,t_0} = \mathbf{w}_j \quad \text{and} \quad \lambda_j^S(t, t_0) = \int_{t_0}^t \lambda_j(s) ds. \quad (46)$$

*Proof.* Since the solution of (43) with the initial condition  $X_{t_0}(\omega) = \mathbf{x}$  is given by

$$X_t(\omega) = \Phi(t, t_0) \left( \mathbf{x} + \sum_{i=1}^r \int_{t_0}^t \Phi^{-1}(s, t_0) b^i(s) dW_s^i \right), \quad (47)$$

we have

$$\begin{aligned} \mathcal{K}^{S,t,t_0} \phi_j^{S,t,t_0}(\mathbf{x}) &= \mathbb{E}_\Omega \left[ \phi_j^{S,t,t_0}(X_t(\omega)) \right] \\ &= \mathbb{E}_\Omega \left[ \langle \Phi(t, t_0) \mathbf{x}, \hat{\mathbf{w}}_j^{t,t_0} \rangle + \left\langle \sum_{i=1}^r \int_{t_0}^t \Phi(t, t_0) \Phi^{-1}(s, t_0) b^i(s) dW_s^i, \hat{\mathbf{w}}_j^{t,t_0} \right\rangle \right] \\ &= \langle \Phi(t, t_0) \mathbf{x}, \hat{\mathbf{w}}_j^{t,t_0} \rangle + \sum_{i=1}^r \left\langle \mathbb{E}_\Omega \left[ \int_{t_0}^t \Phi(t, t_0) \Phi^{-1}(s, t_0) b^i(s) dW_s^i \right], \hat{\mathbf{w}}_j^{t,t_0} \right\rangle \\ &= \mu_j^{t,t_0} \langle \mathbf{x}, \hat{\mathbf{w}}_j^{t,t_0} \rangle = e^{\hat{\lambda}_j(t,t_0)} \phi_j^{S,t,t_0}(\mathbf{x}), \end{aligned} \quad (48)$$

where we used the fact  $\mathbb{E}_\Omega \left[ \int_{t_0}^t \Phi(t, t_0) \Phi^{-1}(s, t_0) b^i(s) dW_s^i \right] = 0$ . With this we proved the first statement.

Since in the commutative case the fundamental matrix can be expressed in the form  $\Phi(t, t_0) = e^{\int_{t_0}^t \mathbf{A}(s) ds}$ , its eigenvectors coincide with the eigenvectors of the matrix  $\mathbf{A}(t)$  and eigenvalues are given by (46).  $\square$

**Proposition 6.** *Let the linear SDE with multiplicative noise be defined by*

$$dX_t = \mathbf{A}(t) X_t dt + \sum_{i=1}^r \mathbf{B}^i(t) X_t dW_t^i, \quad (49)$$

where  $\mathbf{A}(t)$ ,  $\mathbf{B}^i(t)$ ,  $i = 1, \dots, r$  are  $d \times d$  matrices of functions. Denote with  $\Phi(t, t_0)$  the fundamental matrix satisfying the matrix SDE

$$d\Phi = \mathbf{A}\Phi dt + \sum_{i=1}^r \mathbf{B}^i(t) \Phi dW_t^i, \quad \Phi(t_0) = \mathbf{I} \quad (50)$$

and assume that  $\hat{\Phi}(t, t_0) = \mathbb{E}_\Omega [\Phi(t, t_0)]$  is diagonalizable, with simple eigenvalues  $\hat{\mu}_j^{t,t_0} = e^{\hat{\lambda}_j(t,t_0)}$  and left eigenvectors  $\hat{\mathbf{w}}_j^{t,t_0}$ ,  $j = 1, \dots, d$ . Then

$$\phi_j^{S,t,t_0}(\mathbf{x}) = \langle \mathbf{x}, \hat{\mathbf{w}}_j^{t,t_0} \rangle, \quad j = 1, \dots, d, \quad (51)$$

are the eigenfunctions of the stochastic Koopman operator  $\mathcal{K}^{S,t,t_0}$ , with corresponding eigenvalues

$$\lambda_j^S(t, t_0) = \hat{\lambda}_j(t, t_0).$$

If the matrices  $\mathbf{A}(t), \mathbf{B}^i(t), i = 1, \dots, r$  commute, i.e. if  $\mathbf{A}(t)\mathbf{A}(s) = \mathbf{A}(s)\mathbf{A}(t)$ ,  $\mathbf{A}(t)\mathbf{B}^i(s) = \mathbf{B}^i(s)\mathbf{A}(t)$ ,  $\mathbf{B}^i(t)\mathbf{B}^j(s) = \mathbf{B}^j(s)\mathbf{B}^i(t)$  for  $i, j = 1, \dots, r$  and all  $s, t$ , and if the matrices  $\mathbf{A}(t)$  are diagonalizable with the simple eigenvalues  $\lambda_j(t)$  and corresponding left eigenvectors  $\mathbf{w}_j, j = 1, \dots, d$ , then

$$\hat{\mathbf{w}}_j^{t,t_0} = \mathbf{w}_j \quad \text{and} \quad \lambda_j^S(t, t_0) = \int_{t_0}^t \lambda_j(s) ds. \quad (52)$$

*Proof.* For the fundamental matrix  $\Phi(t, t_0)$  and the initial condition  $X_{t_0}(\omega) = \mathbf{x}$ , the solution of (49) is equal to

$$X_t(\omega) = \Phi(t, t_0)\mathbf{x}, \quad (53)$$

thus

$$\begin{aligned} \mathcal{K}^{S,t,t_0} \phi_j^{S,t,t_0}(\mathbf{x}) &= \mathbb{E}_\Omega \left[ \phi_j^{S,t,t_0}(X_t(\omega)) \right] = \mathbb{E}_\Omega \left[ \langle \Phi(t, t_0)\mathbf{x}, \hat{\mathbf{w}}_j^{t,t_0} \rangle \right] \\ &= \langle \hat{\Phi}(t, t_0)\mathbf{x}, \hat{\mathbf{w}}_j^{t,t_0} \rangle = \mu_j^{t,t_0} \langle \mathbf{x}, \hat{\mathbf{w}}_j^{t,t_0} \rangle = e^{\lambda_j(t,t_0)} \phi_j^{S,t,t_0}(\mathbf{x}), \end{aligned} \quad (54)$$

For the case with commutative matrices  $\mathbf{A}(t)$  and  $\mathbf{B}^i(t), i = 1, \dots, r$ , the fundamental matrix  $\Phi(t, t_0)$  can be expressed in an explicit form as

$$\Phi(t, t_0) = e^{\int_{t_0}^t \left( \mathbf{A}(s) - \frac{1}{2} \sum_{i=1}^r \mathbf{B}^i(s) \mathbf{B}^i(s)^T \right) ds + \int_{t_0}^t \sum_{i=1}^r \mathbf{B}^i(s) dW_s^i}. \quad (55)$$

Since

$$\begin{aligned} \hat{\Phi}(t, t_0) &= \mathbb{E}_\Omega \left[ \hat{\Phi}(t, t_0) \right] = e^{\int_{t_0}^t \left( \mathbf{A}(s) - \frac{1}{2} \sum_{i=1}^r \mathbf{B}^i(s) \mathbf{B}^i(s)^T \right) ds} \mathbb{E}_\Omega \left[ e^{\int_{t_0}^t \sum_{i=1}^r \mathbf{B}^i(s) dW_s^i} \right] \\ &= e^{\int_{t_0}^t \left( \mathbf{A}(s) - \frac{1}{2} \sum_{i=1}^r \mathbf{B}^i(s) \mathbf{B}^i(s)^T \right) ds} e^{\int_{t_0}^t \frac{1}{2} \sum_{i=1}^r \mathbf{B}^i(s) \mathbf{B}^i(s)^T ds} = e^{\int_{t_0}^t \mathbf{A}(s) ds}, \end{aligned} \quad (56)$$

the eigenvectors of  $\hat{\Phi}(t, t_0)$  coincide with the eigenvectors of the matrix  $\mathbf{A}(t)$  and eigenvalues are given by (52), which proves the statement. Here we used the fact that  $\mathbb{E}_\Omega \left[ e^{\int_{t_0}^t \mathbf{B}(s) dW_s} \right] = e^{\frac{1}{2} \int_{t_0}^t \mathbf{B}(s) \mathbf{B}(s)^T ds}$ .  $\square$

### 2.3.1 Properties of spectral objects of the stochastic Koopman operators of RDS driven by autonomous SDE.

In what follows, we limit our consideration to the autonomous system of the form (39) where  $G(t, X) = G(X)$  and  $\sigma(t, X) = \sigma(X)$ . In that case the stochastic differential equation generates the one-parameter family of RDS  $\varphi(t, \omega) := \varphi(t, 0, \omega) = \varphi(t + t_0, t_0, \omega)$ , so that the corresponding stochastic Koopman operator family and the associated stochastic eigenvalues and eigenfunctions depend on parameter  $t$ , only. In this autonomous setting, we denote with  $X_t(\mathbf{x})$  the solution of equation (39) for the initial condition  $X_0(\omega) = \mathbf{x}$ , so that according to (40) we have

$$X_t(\mathbf{x}) = \mathbf{x} + \int_0^t G(X_s) ds + \int_0^t \sigma(X_s) dW_s. \quad (57)$$

Since the solution (57) of SDE is a Markov process, which generate an invariant product probability measure, a family of Koopman operators  $\mathcal{K}^{S,t}$  is a semigroup and therefore we can determine its generator  $\mathcal{K}^S$ .

For simplicity, let focus first on the scalar case ( $d = 1$ ). The action of the generator  $\mathcal{K}^S$  can be determined as the limit of the action of the stochastic Koopman operators, thus for smooth enough observable function  $f : M \rightarrow \mathbb{C}$ , we derive it as in [9]:

$$\begin{aligned}
\lim_{t \rightarrow 0+} \frac{\mathcal{K}^{S,t} f(x) - f(x)}{t} &= \lim_{t \rightarrow 0+} \frac{\mathbb{E}_\Omega[f(X_t(x))] - f(x)}{t} \\
&= \lim_{t \rightarrow 0+} \frac{\mathbb{E}_\Omega \left[ f(x) + \int_0^t f'(X_s) dX_s + \int_0^t \frac{1}{2} f''(X_s) \sigma(X_s)^2 ds \right] - f(x)}{t} \\
&= \lim_{t \rightarrow 0+} \frac{1}{t} \mathbb{E}_\Omega \left[ \int_0^t f'(X_s) G(X_s) ds + \int_0^t f'(X_s) \sigma(X_s) dW_s + \int_0^t \frac{1}{2} f''(X_s) \sigma(X_s)^2 ds \right] \\
&= G(X_0) f'(X_0) + \frac{1}{2} f''(X_0) \sigma(X_0)^2 = G(x) f'(x) + \frac{1}{2} \sigma(x)^2 f''(x). \tag{58}
\end{aligned}$$

Here we applied the Itô's formula and use the fact that  $\mathbb{E}_\Omega \left[ \int_0^t f'(X_s) \sigma(X_s) dW_s \right] = 0$ . The obtained differential operator is the generator of the stochastic Koopman family  $\mathcal{K}^{S,t}$ . In multidimensional case it can be determined in a similar way. Thus, we have the following proposition.

**Proposition 7.** *The action of the generator of the stochastic Koopman family  $\mathcal{K}^S$  is given by*

$$\mathcal{K}^S f(\mathbf{x}) = G(\mathbf{x}) \nabla f(\mathbf{x}) + \frac{1}{2} \text{Tr}(\sigma(\mathbf{x})(\nabla^2 f(\mathbf{x}))\sigma(\mathbf{x})^T), \tag{59}$$

where  $\text{Tr}$  denotes the trace of the matrix.

**Proposition 8.** *Let  $\phi$  be an eigenfunction of the stochastic Koopman generator  $\mathcal{K}^S$  associated to RDS driven by an autonomous SDE with the corresponding eigenvalue  $\lambda$ . Then*

$$d\phi(X_t) = \lambda\phi(X_t)dt + \nabla\phi(X_t)\sigma(X_t)dW_t. \tag{60}$$

$\phi$  is the eigenfunction of the stochastic Koopman operator  $\mathcal{K}^{S,t}$  also, i.e.

$$\mathcal{K}^{S,t}\phi(\mathbf{x}) = e^{\lambda t}\phi(\mathbf{x}). \tag{61}$$

*Proof.* Suppose  $d = 1$ . Based on Ito's lemma, the eigenfunction  $\phi(X_t)$  evolves according to

$$\begin{aligned}
d\phi(X_t) &= \phi'(X_t)G(X_t)dt + \frac{1}{2}\phi''(X_t)\sigma(X_t)^2dt + \phi'(X_t)\sigma(X_t)dW_t \\
&= \mathcal{K}^S\phi(X_t)dt + \phi'(X_t)\sigma(X_t)dW_t \\
&= \lambda\phi(X_t)dt + \phi'(X_t)\sigma(X_t)dW_t, \tag{62}
\end{aligned}$$

where in the last equality we used that  $\mathcal{K}^S\phi(x) = \lambda\phi(x)$ . For the initial condition  $X_0(\omega) = x$ , from (62) by using Itô's formula, we get

$$\phi(X_t) = e^{\lambda t}\phi(x) + \int_0^t e^{\lambda(t-s)}\phi'(X_s)\sigma(X_s)dW_s. \tag{63}$$



Then, by using the martingale property  $\mathbb{E}_\Omega \left[ \int_0^t e^{\lambda(t-s)} \phi'(X_s) \sigma(X_s) dW_s \right] = 0$ , we obtain

$$\mathbb{E}_\Omega [\phi(X_t)] = e^{\lambda t} \mathbb{E}_\Omega [\phi(x)] = e^{\lambda t} \phi(x). \quad (64)$$

The left hand side of the obtained equation is equal to  $\mathcal{K}^{S,t} \phi(x)$ , thus we have

$$\mathcal{K}^{S,t} \phi(x) = e^{\lambda t} \phi(x). \quad (65)$$

Using definition (24), we conclude that  $\phi(x)$  is the eigenfunction of the stochastic Koopman operator  $\mathcal{K}^{S,t}$ , with the corresponding eigenvalue  $\lambda^S(t) = \lambda t$ .

By using the similar procedure, the equations (60) and (61) valid in multidimensional case are easily derived.  $\square$

On the other hand, if there exists a function  $\phi(x)$ , which is the eigenfunction of each Koopman operator family member such that for any  $t$  (61) is valid, then  $\phi(x)$  is the eigenfunction of the Koopman generator also. We utilize this fact in some test examples considered in Section 4, in which we use the known eigenfunctions of the Koopman generator to estimate the accuracy of the numerically determined eigenfunctions of the Koopman operators  $\mathcal{K}^{S,t}$ .

The fact that the evolution of the eigenfunctions related to the generator of dynamical system, which actually coincides with the Koopman generator (59), is given by (62), is used in [29]. In that paper the approximations of eigenfunctions computed via diffusion maps are used to parametrize the state of the RDS using the linear operator similarly as in Koopman framework.

**Remark 5.** *Unlike in the case of RDS driven by the RDE, the product of eigenfunctions of the stochastic Koopman generator associated to RDS driven by SDE is not necessarily an eigenfunction. This easily follows from Proposition 7. However, the eigenfunctions in many cases satisfy a recurrence relationship (e.g. Hermite polynomials) and thus can be deduced from the principal eigenfunctions. This reduces the problem to analysis of principal eigenfunctions, and thus  $n$  objects in an  $n$  dimensional space, remarkable for a nominally infinite-dimensional representation.*

### 3 Numerical approximations of the stochastic Koopman operator

We want to explore the possibility of applying the numerical DMD algorithm originally developed for deterministic dynamical systems to the stochastic Koopman operator and to derive the related spectral decomposition numerically. Here we use the enhanced DMD algorithm, proposed in [5], which we denote hereafter by DMD RRR. We briefly describe the algorithm and propose two approaches for applying it to RDS: the standard DMD approach using snapshot pairs, and the DMD applied to the Hankel matrix, where time-delayed snapshots are used.

### 3.1 The DMD RRR algorithm for RDS

Let  $\mathbf{f} = (f_1, \dots, f_n)^T : M \rightarrow \mathbb{C}^n$  be a vector valued observable on the state space. For an  $\mathbf{x} \in M$ , let  $\mathbf{f}^k(\omega, \mathbf{x}) = \mathbf{f} \circ T^{k-1}(\omega, \mathbf{x})$ ,  $k = 1, 2, \dots$  be a vector-valued observable series on the trajectory of the considered discrete-time RDS. Denote its expectation with  $\mathbf{f}^k = \mathbb{E}_\Omega[\mathbf{f}^k(\omega, \mathbf{x})] = \mathcal{K}^{S,k} \mathbf{f}(\mathbf{x})$ . For the continuous-time RDS  $\varphi$ , we choose the time step  $\Delta t$  and define the values of the observables in a same way as in discrete-time case by taking  $T(\omega, \mathbf{x}) = \varphi(\Delta t, \omega) \mathbf{x}$ . The value of the observable at the  $k$ -th step is its value at time moment  $t_k = k\Delta t$  and is evaluated as  $\mathbf{f}^k = \mathcal{K}_{\Delta t}^{S,k} \mathbf{f}(\mathbf{x})$ , where  $\mathcal{K}_{\Delta t}^S$  is the Koopman operator describing the evolution of the RDS at one numerical step, i.e.  $\mathcal{K}_{\Delta t}^S \mathbf{f}(\mathbf{x}) = \mathbb{E}_\Omega[\mathbf{f}(\varphi(\Delta t, \omega) \mathbf{x})]$ .

Let  $\mathbb{K}$  denote the approximation of the Koopman operator by a finite-dimensional matrix. Its action on the range  $\mathbf{X}_m = [\mathbf{f}^0 \ \mathbf{f}^1 \ \dots \ \mathbf{f}^{m-1}]$  should be equal to  $\mathbf{Y}_m = [\mathbf{f}^1 \ \mathbf{f}^2 \ \dots \ \mathbf{f}^m]$ . As already stated, the goal of the numerical algorithms for evaluating the Koopman decomposition is to determine the spectrum and associated eigenvectors of the finite dimensional linear operator  $\mathbb{K}$ . The DMD RRR algorithm used in this work starts in the same way as other SVD-based DMD algorithms, i.e. with the SVD decomposition for low dimensional approximation of data:  $\mathbf{X}_m = \mathbf{U} \mathbf{\Sigma} \mathbf{V}^* \approx \mathbf{U}_k \mathbf{\Sigma}_k \mathbf{V}_k^*$ , where  $\mathbf{\Sigma} = \text{diag}((\sigma_i)_{i=1}^{\min(m,n)})$ ,  $\sigma_i$  are singular values arranged in the descending order, i.e.  $\sigma_1 \geq \dots \geq \sigma_{\min(m,n)} \geq 0$  and  $k$  is the dimension of the approximation space. Then  $\mathbf{Y}_m$  can be approximated as

$$\mathbf{Y}_m \approx \mathbb{K} \mathbf{X}_m \approx \mathbb{K} \mathbf{U}_k \mathbf{\Sigma}_k \mathbf{V}_k^*. \quad (66)$$

Each eigenpair  $(\lambda, \mathbf{v})$  of the Rayleigh quotient  $\mathbf{S}_k = \mathbf{U}_k^* \mathbb{K} \mathbf{U}_k = \mathbf{U}_k^* \mathbf{Y}_m \mathbf{V}_k \mathbf{\Sigma}_k^{-1}$  with respect to the range  $\mathbf{U}_k$ , generates the corresponding Ritz pair  $(\lambda, \mathbf{U}_k \mathbf{v})$ , that is a candidate for the approximation of the eigenvalue and eigenvector of the Koopman operator.

Here we emphasize few crucial points at which the DMD RRR algorithm is improved in comparison with standard DMD algorithms ([26, 36]). The first point refers to the dimension  $k$  of the reduction space. Instead of defining the dimension of the space a priori or to take into account the spectral gap in singular values, [5] proposes to take into account user supplied tolerance  $\varepsilon$ , which is used for defining the dimension  $k$  of the bases. The value of  $k$  is determined as the largest index such that  $\sigma_k \geq \sigma_1 \varepsilon$ . The algorithm is additionally enhanced with the residual computation for each Ritz vector, so that the vectors at which the required accuracy is not attained are not taken into account. The final improvement compared to the standard algorithms refers to scaling of the initial data i.e. if the matrix  $D_x$  is defined with  $D_x = \text{diag}(\|\mathbf{X}_m(:, i)\|_2)_{i=0}^{m-1}$ , where  $\|\cdot\|_2$  stands for  $L_2$  norm of columns of the matrix  $\mathbf{X}_m$ , we set  $\mathbf{X}_m = \mathbf{X}_m^{(1)} D_x$  and  $\mathbf{Y}_m = \mathbf{Y}_m^{(1)} D_x$  and proceed with  $\mathbf{X}_m^{(1)}$  and  $\mathbf{Y}_m^{(1)}$  as data matrices.

### 3.2 Stochastic Hankel DMD RRR algorithm

We use the Hankel DMD method described in [1] for deterministic dynamical system. The Hankel matrix in the stochastic framework is defined as follows. For a scalar observable  $f : M \rightarrow \mathbb{C}$ , we define the vector of  $m+1$  observations along the trajectory that starts at  $\mathbf{x} \in M$  and is driven by a discrete random map  $T$ :

$$\mathbf{f}_m(\omega, \mathbf{x}) = (f(\mathbf{x}), f \circ T(\omega, \mathbf{x}), \dots, f \circ T^m(\omega, \mathbf{x})). \quad (67)$$

For the vector  $\mathbf{f}_m(\mathbf{x})$  denoting the expectation of  $\mathbf{f}_m(\omega, \mathbf{x})$  we have

$$\begin{aligned}\mathbf{f}_m(\mathbf{x}) &= \mathbb{E}_\Omega [\mathbf{f}_m(\omega, \mathbf{x})] = (f(\mathbf{x}), \mathbb{E}_\Omega [f \circ T(\omega, \mathbf{x})], \dots, \mathbb{E}_\Omega [f \circ T^m(\omega, \mathbf{x})]) \\ &= (f(\mathbf{x}), \mathcal{K}^S f(\mathbf{x}), \dots, \mathcal{K}^{S,m} f(\mathbf{x})).\end{aligned}\quad (68)$$

The Hankel matrix evaluated along the trajectory starting at  $\mathbf{x} \in M$ , generated by the map  $T$  is defined by

$$\begin{aligned}\mathbf{H}^S(\omega, \mathbf{x}) &= [\mathbf{f}_m(\omega, \mathbf{x}) \ \mathbf{f}_m \circ T(\omega, \mathbf{x}) \ \dots \ \mathbf{f}_m \circ T^{n-1}(\omega, \mathbf{x})]^T \\ &= \begin{pmatrix} f(\mathbf{x}) & f \circ T(\omega, \mathbf{x}) & \dots & f \circ T^m(\omega, \mathbf{x}) \\ f \circ T(\omega, \mathbf{x}) & f \circ T^2(\omega, \mathbf{x}) & \dots & f \circ T^{m+1}(\omega, \mathbf{x}) \\ \vdots & \vdots & \ddots & \vdots \\ f \circ T^{n-1}(\omega, \mathbf{x}) & f \circ T^n(\omega, \mathbf{x}) & \dots & f \circ T^{m+n-1}(\omega, \mathbf{x}) \end{pmatrix}.\end{aligned}\quad (69)$$

We define the expected Hankel matrix as  $\mathbf{H}^S(\mathbf{x}) = \mathbb{E}_\Omega [\mathbf{H}^S(\omega, \mathbf{x})]$ . By using (68) and (69) we get

$$\begin{aligned}\mathbf{H}^S(\mathbf{x}) &= \mathbb{E}_\Omega [\mathbf{H}^S(\omega, \mathbf{x})] = [\mathbf{f}_m(\mathbf{x}) \ \mathcal{K}^S \mathbf{f}_m(\mathbf{x}) \ \dots \ \mathcal{K}^{S,n-1} \mathbf{f}_m(\mathbf{x})]^T \\ &= \begin{pmatrix} f(\mathbf{x}) & \mathcal{K}^S f(\mathbf{x}) & \dots & \mathcal{K}^{S,m} f(\mathbf{x}) \\ \mathcal{K}^S f(\mathbf{x}) & \mathcal{K}^{S,2} f(\mathbf{x}) & \dots & \mathcal{K}^{S,m+1} f(\mathbf{x}) \\ \vdots & \vdots & \ddots & \vdots \\ \mathcal{K}^{S,n-1} f(\mathbf{x}) & \mathcal{K}^{S,n} f(\mathbf{x}) & \dots & \mathcal{K}^{S,m+n-1} f(\mathbf{x}) \end{pmatrix}.\end{aligned}\quad (70)$$

Note that the rows of  $\mathbf{H}^S(\mathbf{x})$  are approximations of functions in the Krylov subspace

$$\mathbb{K}_n(\mathcal{K}^S, f) = (f \ \mathcal{K}^S f \ \dots \ \mathcal{K}^{S,n-1} f) \quad (71)$$

obtained by sampling values of functions  $\mathcal{K}^{S,j} f$ ,  $j = 0, \dots, n-1$  along the trajectory starting at  $x \in M$ .

As described previously, when we consider the continuous-time RDS, we could associate to it a discrete RDS by defining the one-step map by

$$T(\omega, \mathbf{x}) = \varphi(\Delta t, \omega) \mathbf{x}$$

for the chosen  $\Delta t$ . Then, in (68) and (70) the Koopman operator  $\mathcal{K}^S$  should be replaced with the operator  $\mathcal{K}_{\Delta t}^S$ .

In application of DMD RRR algorithm to Hankel matrix, the data matrix  $\mathbf{X}_m$  is defined by taking the first  $m$  columns of the Hankel matrix  $\mathbf{H}^S(\omega, \mathbf{x})$  and the data matrix  $\mathbf{Y}_m$  is defined by taking the last  $m$  columns of  $\mathbf{H}^S(\omega, \mathbf{x})$ . We refer to this procedure as to the stochastic Hankel DMD RRR algorithm.

### 3.3 Convergence of the stochastic Hankel DMD RRR algorithm

It was proved in [1] that for ergodic systems the eigenvalues and eigenvectors obtained by the extended DMD algorithm used on the Hankel matrix, converge to the true Koopman eigenvalues and eigenfunctions of considered system, under the assumption that observables are in an invariant subspace of the Koopman operator. The convergence of the

DMD algorithm to the eigenvalues and the eigenfunctions of the Koopman operator is proved in [29] for the class of RDS in which the noise is modeled by independent identically distributed random variables, under the assumption of ergodicity and the existence of the finite dimensional invariant subspace. Under the similar assumptions, but for a more general class of RDS, we prove that the convergence is accomplished for DMD RRR algorithm in the stochastic case. Our proof is based on the fact that the eigenvalues and the eigenfunctions obtained by DMD RRR algorithm correspond to the matrix that is similar to the companion matrix, which represents the finite dimensional approximation of the Koopman operator in the Krylov basis.

**Proposition 9.** *Suppose that the dynamics on the compact invariant set  $A \subseteq M$  is given by the a map  $T(\omega, \cdot) : A \rightarrow A$  for each  $\omega \in \Omega$ . Assume that  $T$  is ergodic on  $\Omega \times A$  with respect to some invariant measure  $\nu$ . Let the Krylov subspace  $\mathbb{K}_n(\mathcal{K}^S, f)$  span an  $r$ -dimensional subspace of the Hilbert space  $\mathcal{H} = L^2(A, \mu)$ , with  $r < n$ . Then for almost every  $\mathbf{x} \in A$ , as  $m \rightarrow \infty$ , the eigenvalues and eigenfunctions obtained by using the stochastic Hankel DMD RRR algorithm converge to the true eigenvalues and eigenfunctions of the stochastic Koopman operator.*

*Proof.* Consider the observables  $f : A \rightarrow \mathbb{R}$  belonging to the Hilbert space  $\mathcal{H}$ , where  $\mu = \mathbb{E}_\Omega(\nu)$ . Birkhoff's ergodic theorem states that the time average of  $f$  under  $T$  exists for a.e.  $(\omega, \mathbf{x})$ . Under assumption that the RDS driven by  $T$  is ergodic, the time average is given by

$$\lim_{m \rightarrow \infty} \frac{1}{m} \sum_{k=0}^{m-1} f \circ T^k(\omega, \mathbf{x}) = \int_{\Omega \times A} f d\nu, \quad \text{a. e. on } \Omega \times A. \quad (72)$$

As a consequence we obtain

$$\mathbb{E}_\Omega \left[ \lim_{m \rightarrow \infty} \frac{1}{m} \sum_{k=0}^{m-1} f \circ T^k(\omega, \mathbf{x}) \right] = \int_A f d\mu, \quad \text{a. e. on } A. \quad (73)$$

For observables  $f, g \in \mathcal{H}$  let the vectors of  $m$  observations along the trajectory starting at  $\mathbf{x} \in A$  of the RDS driven by the map  $T$  be denoted by  $\mathbf{f}_{m-1}(\omega, \mathbf{x})$  and  $\mathbf{g}_{m-1}(\omega, \mathbf{x})$  and defined by (67). If we denote the data-driven inner product by  $\langle \mathbf{f}_{m-1}(\omega, \mathbf{x}), \mathbf{g}_{m-1}(\omega, \mathbf{x}) \rangle$ , we have

$$\begin{aligned} \lim_{m \rightarrow \infty} \frac{1}{m} \mathbb{E}_\Omega [\langle \mathbf{f}_{m-1}(\omega, \mathbf{x}), \mathbf{g}_{m-1}(\omega, \mathbf{x}) \rangle] &= \lim_{m \rightarrow \infty} \frac{1}{m} \mathbb{E}_\Omega \left[ \sum_{k=0}^{m-1} (f \circ T^k(\omega, \mathbf{x})) (g^* \circ T^k(\omega, \mathbf{x})) \right] \\ &= \lim_{m \rightarrow \infty} \frac{1}{m} \sum_{k=0}^{m-1} \mathbb{E}_\Omega [f g^* (T^k(\omega, \mathbf{x}))] = \int_A f g^* d\mu = \langle f, g \rangle_{\mathcal{H}}. \end{aligned} \quad (74)$$

Using the assumption that  $\mathbb{K}_n(\mathcal{K}^S, f)$  spans  $r$ -dimensional subspace of  $\mathcal{H}$ , we can reduce the study of the Koopman operator to this subspace. Consider the Hankel matrix  $\mathbf{H}^S(\omega, \mathbf{x})$  of dimension  $r \times (m+1)$  along a trajectory starting at  $\mathbf{x}$ . The DMD RRR algorithm is then applied to  $\mathbf{X}_m = [\mathbf{f}_{m-1}(\omega, \mathbf{x}) \ \mathbf{f}_{m-1} \circ T(\omega, \mathbf{x}) \ \dots \ \mathbf{f}_{m-1} \circ T^{r-1}(\omega, \mathbf{x})]^T$  and

$\mathbf{Y}_m = [\mathbf{f}_{m-1} \circ T(\omega, \mathbf{x}) \dots \mathbf{f}_{m-1} \circ T^r(\omega, \mathbf{x})]^T$ . We denote by  $\tilde{\mathbf{C}}$  the companion matrix

$$\tilde{\mathbf{C}} = \begin{pmatrix} 0 & 0 & \dots & 0 & \tilde{c}_0 \\ 1 & 0 & \dots & 0 & \tilde{c}_1 \\ 0 & 1 & \dots & 0 & \tilde{c}_2 \\ \vdots & \vdots & \ddots & \vdots & \vdots \\ 0 & 0 & \dots & 1 & \tilde{c}_{r-1} \end{pmatrix}. \quad (75)$$

Since the matrix  $\mathbf{X}_m$  has a full row rank, the pseudoinverse is of the form  $\mathbf{X}_m^\dagger = \mathbf{X}_m^* (\mathbf{X}_m \mathbf{X}_m^*)^{-1}$  and the matrix  $\tilde{\mathbf{C}}$  is equal

$$\tilde{\mathbf{C}} = \mathbf{Y}_m \mathbf{X}_m^\dagger = \mathbf{Y}_m \mathbf{X}_m^* (\mathbf{X}_m \mathbf{X}_m^*)^{-1} = \left( \frac{1}{m} \mathbf{Y}_m \mathbf{X}_m^* \right) \left( \frac{1}{m} \mathbf{X}_m \mathbf{X}_m^* \right)^{-1} = \left( \frac{1}{n} \mathbf{Y}_m \mathbf{X}_m^* \right) \tilde{\mathbf{G}}^{-1}. \quad (76)$$

Here  $\tilde{\mathbf{G}}$  denotes the numerical Grammian matrix whose elements are equal to

$$\tilde{\mathbf{G}}_{ij}(\omega, \mathbf{x}) = \frac{1}{m} \langle \mathbf{f}_{m-1} \circ T^{i-1}(\omega, \mathbf{x}), \mathbf{f}_{m-1} \circ T^{j-1}(\omega, \mathbf{x}) \rangle, \quad i, j = 1, \dots, r. \quad (77)$$

From (76) we get that the elements in the last column of  $\tilde{\mathbf{C}}$  are equal to

$$\tilde{c}_j(\omega, \mathbf{x}) = \frac{1}{m} \langle \mathbf{f}_{m-1} \circ T^{j-1}(\omega, \mathbf{x}), \mathbf{f}_{m-1} \circ T^r(\omega, \mathbf{x}) \rangle, \quad j = 1, \dots, r. \quad (78)$$

Furthermore, by using (74) and (68) we conclude that

$$\lim_{m \rightarrow \infty} \mathbb{E}_\Omega [\tilde{\mathbf{G}}_{ij}(\omega, \mathbf{x})] = \langle \mathcal{K}^{S, i-1} f, \mathcal{K}^{S, j-1} f \rangle_{\mathcal{H}}, \quad i, j = 1, \dots, r \quad (79)$$

and

$$\lim_{m \rightarrow \infty} \mathbb{E}_\Omega [\tilde{c}_j(\omega, \mathbf{x})] = \langle \mathcal{K}^{S, j-1} f, \mathcal{K}^{S, r} f \rangle_{\mathcal{H}} \quad j = 1, \dots, r. \quad (80)$$

Since the elements on the right hand sides of (79) and (80) are actually elements of the Grammian matrix and the elements in the last column of the companion matrix that represents the action of the Koopman operator restricted to the Krylov subspace  $\mathbb{K}_n(\mathcal{K}^S, f)$ , we conclude that the expectations of the numerical values converge as  $m \rightarrow \infty$  to the corresponding values associated to the exact companion matrix. As in [1], the consequence of previous conclusions is that the eigenvalues of the companion matrix  $\tilde{\mathbf{C}}$  converge to the eigenvalues of the exact companion matrix, i.e. to the exact eigenvalues of the stochastic Koopman operator. Since the eigenvalues and eigenvectors obtained from DMD RRR algorithm correspond to the matrix similar to the companion matrix  $\tilde{\mathbf{C}}$ , the conclusion follows.  $\square$

Thus, under the assumptions of ergodicity on a finite dimensional subspace of space  $\mathcal{H}$  spanned by  $\mathbb{K}_n(\mathcal{K}^S, f)$ , by applying the DMD RRR algorithm to matrix  $\mathbf{H}^S(\omega, \mathbf{x})$ , one could expect to get approximations of the spectral objects of the stochastic Koopman operator.

## 4 Numerical examples.

In this section we illustrate the computation of spectral objects of the stochastic Koopman operator by numerical experiments. In most considered RDS examples, we obtain an analytic expression for the Koopman eigenvalues and eigenfunctions of the related deterministic dynamical system and then explore the behavior of the algorithm on the RDS.

### 4.1 Discrete random dynamical system examples.

#### 4.1.1 Noisy rotation on the circle

Consider the dynamical system defined in Example 1. We use the following set of observables:

$$f_j(x) = \cos(j2\pi x), g_j(x) = \sin(j2\pi x), \quad j = 1, \dots, n_1,$$

arranged in the vector valued observable as

$$\mathbf{f} = (f_1, \dots, f_{n_1}, g_1, \dots, g_{n_1})^T.$$

Let  $x_k$  denote the state value under the flow dynamics at the  $k$ -th step. The values of the observable function evaluated as  $\mathbf{f}^k = \mathbf{f}(x_k)$  are used to form matrices  $\mathbf{X}_m$  and  $\mathbf{Y}_m$  used as inputs in DMD RRR algorithm described in previous section. To recover the spectrum of the stochastic Koopman operator, we consider the values of the observable functions on one long enough trajectory instead of considering its values on multiple trajectories since we can either prove, or we assume, that the considered stochastic process is ergodic. Therefore, in the stochastic case, the same approach as in the deterministic case is used. We take  $n_1 = 150$ , which gives  $n = 300$  observable functions, and use  $m = 5000$  sequential snapshots to determine the matrices  $\mathbf{X}_m$  and  $\mathbf{Y}_m$ . The numerical results for the flow with the parameters  $\theta = \pi/320$  and  $\delta = 0.01$  obtained by using the DMD RRR algorithm are presented in Figure 1. We note that the eigenvalues obtained in the deterministic case lie, as expected, on unit circle. The real parts of eigenfunctions  $\phi_i(x)$ ,  $i = 1, 2, 3$ , which we recover numerically, are presented in subfigure (c) of Figure 1. They closely coincide with the theoretically established eigenfunctions given by (15). The results presented in subfigure (e) of Figure 1 show that numerically captured eigenvalues of the stochastic Koopman operator coincide very well with theoretical eigenvalues (17), which are presented with blue circles in the figure. In the stochastic case, the real parts of the eigenfunctions belonging to the first three eigenvalues  $\lambda_i^S, i = 1, 2, 3$  are presented in subfigure (f) of Figure 1. As shown in Example 1, the eigenfunctions are given by (15). Two remarks are in order: 1) The deterministic and stochastic Koopman operator commute in this case, and thus the eigenfunctions are the same and the addition of noise does not perturb them (cf. [7] where the numerically computed eigenfunctions in a similar commuting situation were not sensitive to the noise introduced in the system). 2) The eigenvalues are computed very accurately, and their real part detected, despite the noise being relatively small. This might be due to the fact that the observables we chose are in eigenspace of the stochastic Koopman operator. Results very similar to the presented ones were obtained when the observable vector is constructed with the observable functions:  $f_j(x) = e^{j2\pi i x}$  and  $g_j(x) = e^{-j2\pi i x}$ ,  $j = 1, \dots, n_1$ .

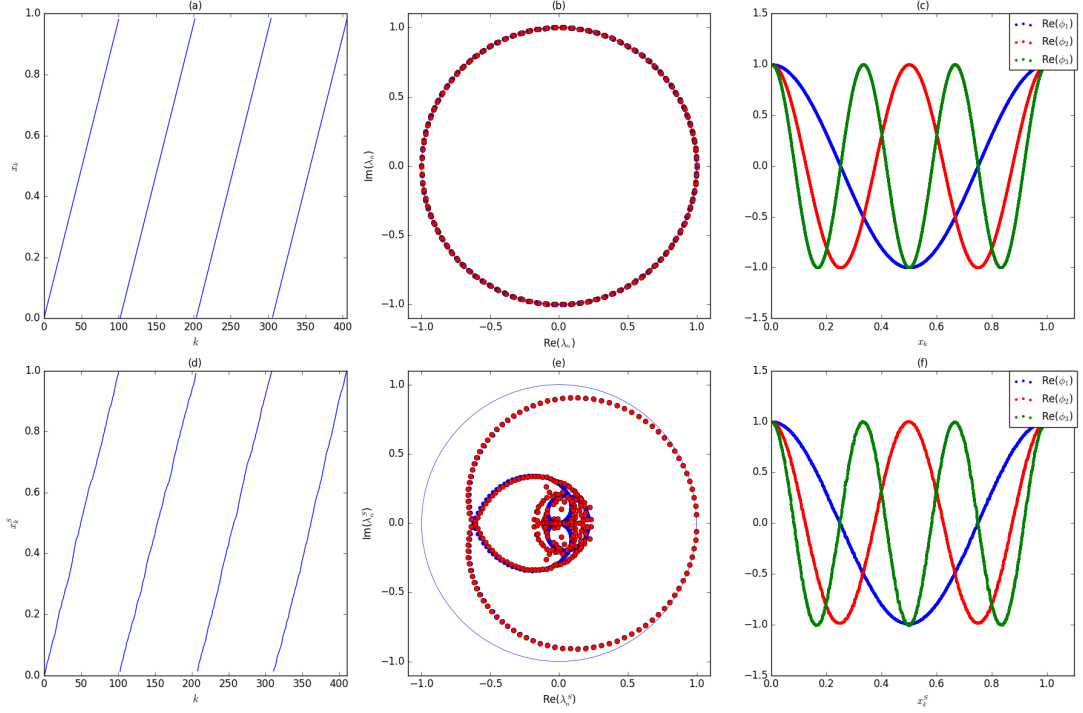


Figure 1: Rotation on circle defined by (12) and (13). Deterministic case  $\theta = \pi/320$ : (a) solution; (b) Koopman eigenvalues; (c) real part of eigenfunctions. Stochastic case  $\theta = \pi/320$ ,  $\delta = 0.01$ : (d) solution; (e) stochastic Koopman eigenvalues; (f) real part of eigenfunctions.

#### 4.1.2 Discrete linear random dynamical system.

Here we consider the discrete linear RDS driven by a map (18) with

$$\mathbf{A}(\omega) = \begin{pmatrix} 0 & \pi(\omega) \\ -\pi(\omega) & 0 \end{pmatrix}, \quad (81)$$

where  $\pi$  is given by (3). The coordinates  $\omega_i$ ,  $i \in \mathbb{Z}^+$  of  $\omega \in \Omega$  are induced by i.i.d. random variables with the following distribution

$$P(\omega_i = 1) = p_1, \quad P(\omega_i = 2) = 1 - p_1, \quad 0 < p_1 < 1.$$

As proved in Proposition 2, the principal eigenvalues of the stochastic Koopman operator are equal to the eigenvalues of the matrix  $\hat{\mathbf{A}} = \mathbb{E}_\Omega[\mathbf{A}(\omega)]$ , while the associated eigenfunctions are given by (19). We take  $p_1 = 0.75$  and select  $N = 10^4$  initial points uniformly distributed over  $[0, 1] \times [0, 1]$ . For every chosen initial point  $\mathbf{x}_{j,0}$ ,  $j = 1, \dots, N$ , we determine the random trajectory  $\mathbf{x}_{j,k}$ ,  $k = 1, 2, \dots$ , where  $\mathbf{x}_{j,k}$  denotes state value at  $k$ -th step. The DMD RRR algorithm is applied to the full-state observables by taking states on each of the trajectory separately, i.e. we take the following matrices as the algorithm input:  $\mathbf{X}_{m,j} = [\mathbf{x}_{j,0}, \mathbf{x}_{j,1}, \dots, \mathbf{x}_{j,m-1}]$  and  $\mathbf{Y}_{m,j} = [\mathbf{x}_{j,1}, \mathbf{x}_{j,2}, \dots, \mathbf{x}_{j,m}]$ ,  $j = 1, \dots, N$ . In every computation we obtain the eigenvalue pair, which should approximate the principal Koopman eigenvalues  $\hat{\lambda}_{1,2}$ . For the chosen set of initial conditions and by varying the parameter  $m$ , we get samples of approximating eigenvalues. The  $L_1$ ,  $L_2$  and  $L_\infty$  norms of

the difference between the exact eigenvalues and the computed eigenvalues are presented in Figure 2. One could notice that the accuracy of the obtained eigenvalues increases monotonically with the number of snapshots  $m$  used in the computations, and that the error is  $\mathcal{O}(\frac{1}{\sqrt{m}})$ , as would be expected for a random process of this type.

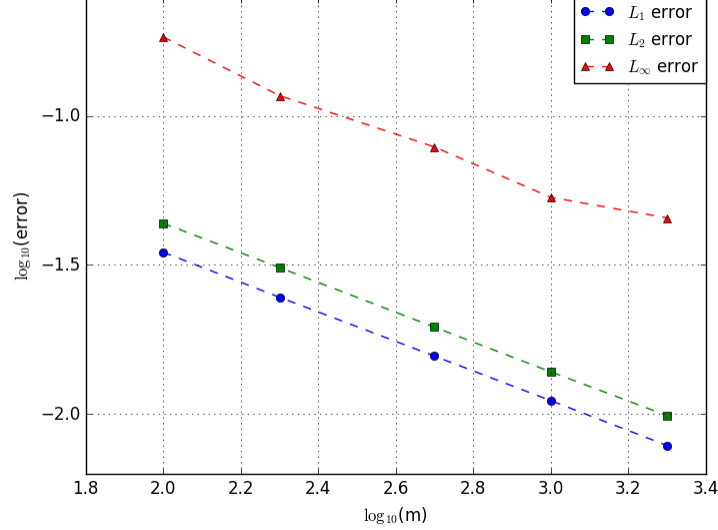


Figure 2: Discrete linear RDS defined by (81).  $L_1$ ,  $L_2$ , and  $L_\infty$  errors of approximated Koopman eigenvalues.

## 4.2 Continuous-time linear random dynamical system.

We consider now the continuous-time linear RDS that evolves according to (25) with

$$\mathbf{A}(\omega) = \begin{pmatrix} \pi(\omega) & 1 \\ -b^2 & \pi(\omega) \end{pmatrix}. \quad (82)$$

The coordinates  $\omega(t)$ ,  $t \in \mathbb{R}^+$  of  $\omega \in \Omega$  are induced by i.i.d. random variables with the following distribution

$$P(\omega(t) = a_1) = p_1, \quad P(\omega(t) = a_2) = 1 - p_1, \quad 0 < p_1 < 1.$$

Note that matrices  $A(\omega)$  commute.

The goal is to determine the spectral decomposition belonging to the stochastic Koopman operator. As described in the previous section, the value of an observable at each time step should be obtained as the expectation of its value after the one time step  $\Delta t$ . In order to approximate these values, we generate for the fixed initial condition  $\mathbf{x}_0$  a large number of trajectories driven by the given RDE and evaluate them at the discretized time moments  $t_k = k\Delta t$ ,  $k = 0, 1, 2, \dots$ . Let denote with  $\mathbf{x}_j(t)$ ,  $j = 1, \dots, N$  the  $j$ -th realization of the solution and its value at  $t_k$  with  $\mathbf{x}_{j,k} = \mathbf{x}_j(t_k)$ . Then the set of  $m + 1$  corresponding snapshots of the  $j$ -th realization at the chosen time moments is given by  $[\mathbf{x}_{j,0} \dots \mathbf{x}_{j,m}]$ . Notice that  $\mathbf{x}_{j,0} = \mathbf{x}_0$  for each  $j$ . Based on the obtained solutions we determine the value of full state observable at the same moments, i.e. we get  $[\mathbf{f}_{j,0} \dots \mathbf{f}_{j,m}]$ .



From the definition of the stochastic Koopman operator

$$\mathcal{K}_{\Delta t}^S \mathbf{f}_{j,k} = \mathbb{E}_{\Omega}[\mathbf{f}_{j,k+1}] \approx \frac{1}{N} \sum_{j=1}^N \mathbf{f}_{j,k+1} \quad (83)$$

If we apply the obtained approximation recursively for each  $k$ , it follows that

$$\mathbf{f}^{k+1} = \mathcal{K}_{\Delta t}^S \mathbf{f}^k \approx \frac{1}{N} \sum_{j=1}^N \mathbf{f}_{j,k+1}.$$

The DMD RRR algorithm described in the previous section is then applied on the matrices formed from the values  $\mathbf{f}^k$ .

It follows from the Proposition 3 that eigenvalues of the stochastic Koopman operator coincide with the eigenvalues of the matrix  $\hat{\mathbf{A}} = \mathbb{E}_{\Omega}[\mathbf{A}(\omega)]$ . In the considered case we have

$$\hat{\mathbf{A}} = \mathbb{E}_{\Omega}[\mathbf{A}(\omega)] = \begin{pmatrix} \hat{a} & 1 \\ -b^2 & \hat{a} \end{pmatrix}, \text{ where } \hat{a} = \sqrt{p_1 a_1 + (1 - p_1) a_2},$$

so that the stochastic Koopman eigenvalues are  $\lambda_{1,2}^S = \hat{a} \mp b i$ .

In the numerical computation we take  $a_1 = -0.1$ ,  $a_2 = 0.1$ , and  $b = 2$  so that  $\hat{a} = 0.1\sqrt{1 - 2p_1}$ . The numerical approximation of the solution of the considered RDE based on  $N = 100$  sampled trajectories and for the values of  $p_1 = 0.25$ ,  $p_1 = 0.5$ , and  $p_1 = 0.75$  are presented in Figure 3. Taking into account  $m = 3000$  snapshots based on the sampled trajectories, we obtain the following numerical approximation of the eigenvalues:  $-0.05014683 \pm 2.00003917 i$ ,  $0.00035214 \pm 1.99996498 i$ ,  $0.05055979 \pm 2.00000085 i$ , which approximate the exact values:  $-0.05 \pm 2 i$ ,  $\pm 2 i$ ,  $0.05 \pm 2 i$  respectively, with the precision greater than  $10^{-3}$ .

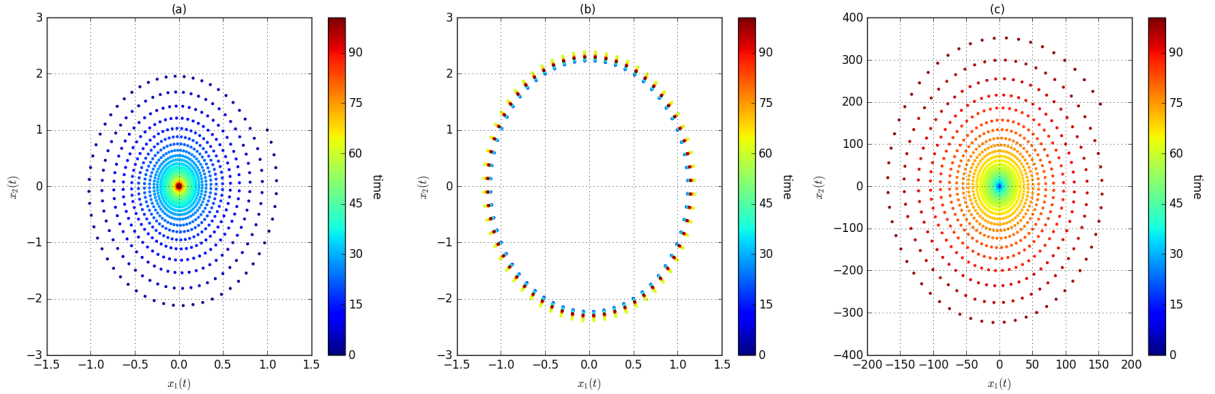


Figure 3: Numerical solutions  $x_1^S(t)$ ,  $x_2^S(t)$  of linear random dynamical system defined by (82) for different values of parameter  $p_1$ : (a)  $p_1 = 0.25$ ; (b)  $p_1 = 0.5$ ; (c)  $p_1 = 0.75$ . The color coding refers to time  $t$ .

### 4.3 Stochastic differential equations examples

In this section we consider the flow induced by the autonomous form of SDE (39) with added random force accounting for the effect of the noise and disturbances of the system.

In the considered examples the numerical solutions are determined by using the Euler-Mayurama method and the Runge-Kutta method for SDE developed in [23]. We use the fact that the convergence of Euler-Maruyama method is, for the examples we consider here, proved in [10], so that with very small time step we obtain the reference solutions and then check the numerical solutions obtained with Runge-Kutta method. Nevertheless, the Runge-Kutta method performs significantly better and needs less computational effort to attain the same accuracy since much larger time step can be used.

#### 4.3.1 Linear scalar differential equation with random force

We consider the following SDE

$$dX = \mu X dt + \sigma dW_t, \quad (84)$$

where  $\mu < 0$  is fixed parameter and  $\sigma > 0$ . It is known that in the deterministic case, i.e. for  $\sigma = 0$ , the Koopman eigenvalues are equal to

$$\lambda_n = n\mu,$$

and the related Koopman eigenfunctions are

$$\phi_n(x) = x^n.$$

In the stochastic case, the spectral properties of the Koopman operator associated to the given equation were studied in [6]. Its eigenvalues are the same as in deterministic case, while the eigenfunctions are (see [6])

$$\phi_n(x) = a_n H_n(\alpha x), \quad \alpha = \sqrt{\frac{|\mu|}{\sigma}}.$$

Here  $a_n$  denotes normalizing parameter and  $H_n$  are Hermite polynomials.

It is known that the accuracy of eigenvalues and eigenfunctions obtained by DMD algorithms is closely related to the choice of observable functions. In the deterministic case, with monomials  $f_j(x) = x^j, j = 1, \dots, n$ , satisfying results for the first  $n$  eigenvalues were obtained for moderate values of  $n$ , for example  $n = 10$ , while for larger values of  $n$  significant numerical errors arise and only a few eigenvalues were captured correctly. That is a consequence of highly ill-conditioned system when monomials of higher order are used since their evolution is given by  $e^{\mu t}x$ . In the case with  $n = 10$  and  $m = 2000$  snapshots, the ten leading eigenvalues are determined with the accuracy greater than 0.01 (see Figure 4(b)). It is worth mentioning that the standard DMD algorithm, which does not include scaling of data, was more sensitive and when it was applied on the same series of snapshots, at most three eigenvalues with the accuracy greater than 0.01 were computed.

In the stochastic case the DMD RRR algorithm was applied on the same set of observable functions as in the deterministic case. For the chosen initial condition, we generate the  $N = 1000$  trajectories to determine the approximations of the expected value of the observable functions, which are then used in DMD RRR algorithm. By using the approximations for expected value of the observables the additional errors are introduced in the system, which then in combination with the stochastic effects lead to more sensitive

computational process. As consequence, in the stochastic case, the number of eigenvalues captured with satisfying accuracy decreases and only three of them are captured with the accuracy greater than  $10^{-2}$  (see Figure 4(e)). The eigenfunctions associated to the three accurate eigenvalues are also captured with satisfying accuracy (Figure 4(f)). The accuracy of the algorithm could be increased by increasing the number of computed trajectories for evaluating the approximations of expected values of the observables.

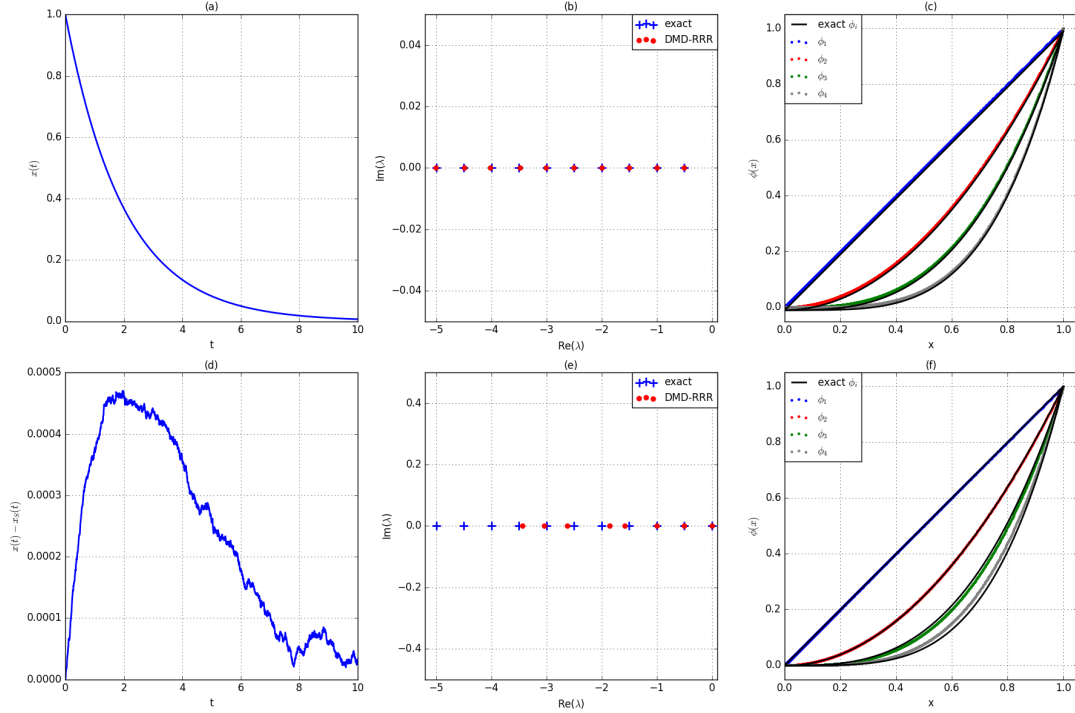


Figure 4: Linear scalar equation (84). Deterministic case  $\mu = -0.5$ : (a) solution; (b) Koopman eigenvalues; (c) Koopman eigenfunctions; Stochastic case  $\mu = -0.5$   $\sigma = 0.001$ : (d) difference between the solutions of deterministic and stochastic equations; (e) stochastic Koopman eigenvalues; (f) stochastic Koopman eigenfunctions.

#### 4.3.2 Pitchfork bifurcation with random force

One of the simplest nonlinear dynamical system describing a bifurcation is given by the one-dimensional equation of the form (39)

$$dX = (\mu X - X^3)dt + \sigma dW_t, \quad (85)$$

where  $\mu$  is a fixed parameter. It is known that the solutions are of different nature for  $\mu > 0$ ,  $\mu = 0$  and  $\mu < 0$  [6]. Here we consider the case  $\mu < 0$ . The Koopman eigenvalues that correspond to the Koopman operator of the deterministic equation, when  $\sigma = 0$ , are as in the linear scalar equation equal to

$$\lambda_n = n\mu,$$

while the associated eigenfunctions are

$$\phi_n(x) = \left( \frac{x}{\sqrt{x^2 + |\mu|}} \right)^n.$$

In the stochastic case, when  $\sigma > 0$ , the eigenvalues and eigenfunctions of the generator of the stochastic Koopman operator family can be evaluated by solving the associated Schrödinger equation (see [6]). We determine their approximations numerically by solving Schrödinger equation using finite difference method. For small values of  $\sigma$  the eigenvalues and eigenfunctions are very similar as in deterministic case.

As in the linear scalar case, we first apply the DMD RRR algorithm to compute the eigenvalues and eigenfunctions of the Koopman operator in the deterministic case. The specific set of observables used in the computation is of importance for the accuracy of the results. When we use the analytically known eigenfunctions or their linear combinations as the observable functions, accurate results, both in eigenvalues and eigenfunctions, are obtained (see Figure 5). In contrast, when the set of observables was composed of monomials, the results were less accurate and only a few leading eigenvalues and eigenfunctions were computed with satisfying accuracy. The agreement is much better in the deterministic than in the stochastic case.

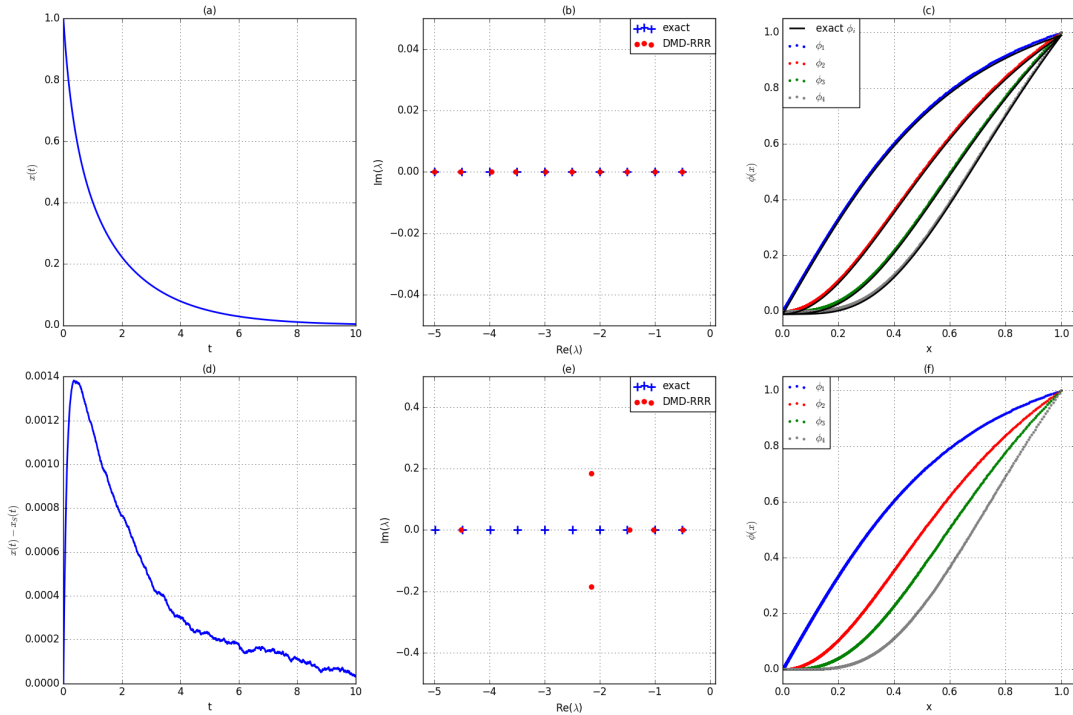


Figure 5: Pitchfork bifurcation equation (85). Deterministic case  $\mu = -0.5$ : (a) solution; (b) Koopman eigenvalues; (c) Koopman eigenfunctions. Stochastic case  $\mu = -0.5$   $\sigma = 0.001$ : (d) difference between the solutions of deterministic and stochastic equations; (e) stochastic Koopman eigenvalues; (f) stochastic Koopman eigenfunctions.

### 4.3.3 Noisy van der Pol oscillator.

We analyze the two-dimensional test example in which the deterministic part is the system of two equations modeling standard Van der Pol oscillator. The stochastic part is modeled by the one-dimensional Wiener process so that the following system is considered

$$\begin{aligned} dX_1 &= X_2 dt \\ dX_2 &= (\mu(1 - X_1^2)X_2 - X_1) dt + \sqrt{2\epsilon} dW_t. \end{aligned} \quad (86)$$

It is proved in [2] that the solution of the considered SDE system exists. Furthermore, it is proved in [10] that the numerical solutions computed with the Euler-Maruyama method converge to the exact solution of the considered SDE, which is also true for the Runge-Kutta method for SDE [23] used here.

As in the previous examples, we consider first the deterministic system. It is well known that the dynamics converge to an asymptotic limit cycle whose basin of attraction is the whole  $\mathbb{R}^2$ . For the parameter value  $\mu = 0.3$  the basic frequency of the limit cycle is  $\omega_0 \approx 0.995$ . For the chosen initial state, the base frequency computed by applying the Hankel DMD RRR algorithm using the scalar observable function  $f(X_1, X_2) = X_1 + X_2 + \sqrt{X_1^2 + X_2^2}$ , is equal to 0.9944151. In Figure 6 we present the eigenvalues computed with the standard DMD algorithm and the eigenvalues obtained by using DMD RRR algorithm for which the residuals of eigenvectors are smaller than the chosen threshold  $\epsilon = 10^{-3}$ . The number of eigenvalues and eigenvectors obtained by using both DMD algorithms is 250 for the chosen Hankel matrix with  $n = 250$  rows and a larger number of columns, but for only few of them the residuals of the eigenvectors computed with DMD RRR algorithm are smaller than the chosen threshold. The eigenvalues obtained using DMD RRR algorithm form a lattice structure containing the eigenvalues of the form  $\{k\omega_0, -\mu + k\omega_0 : k \in \mathbb{Z}\}$ , which is consistent with the theoretical results given in [19]. As nicely visible in Figure 6 the standard DMD algorithm without residue evaluation was not able to distinguish the correctly evaluated spectral elements of the operator. In Figure 7 we present the solution and the eigenvalues for which the residuals of eigenvectors are smaller than the chosen threshold. The time evolution of the real part of the first three eigenfunctions of the Van der Pol system presented in the same figure coincide with the results presented in [1].

The same approach as in deterministic case is applied on the solution obtained from the stochastic system (86). From Figure 7 we can conclude that some sort of stochastic asymptotic limit cycle appears i.e. for large  $t$  the solution is distributed around the deterministic limit cycle, where this distribution depend on the parameter  $\epsilon$ . Despite the fact that the eigenvalues and eigenfunctions of the related stochastic Koopman operator are not known, the numerically determined eigenvalues with the negative real part suggest that the stable RDS is considered. Again, as in the deterministic case, only the eigenvalues for which the corresponding eigenvectors have the residuals smaller than threshold  $\epsilon = 10^{-3}$  are chosen and presented in Figure 7. By comparing the results shown in Figure 7, we conclude that the numerically determined time evolution of eigenfunctions in the stochastic case are very similar to the evolution of eigenfunctions in the deterministic case.

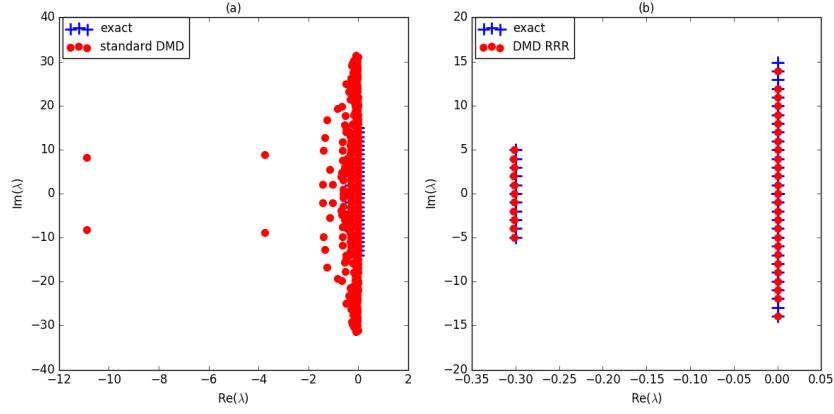


Figure 6: Van der Pol oscillator (86). Deterministic case: (a) eigenvalues obtained by using standard DMD algorithm; (b) eigenvalues obtained by using DMD RRR algorithm with the threshold for the residuals equal to 0.001.

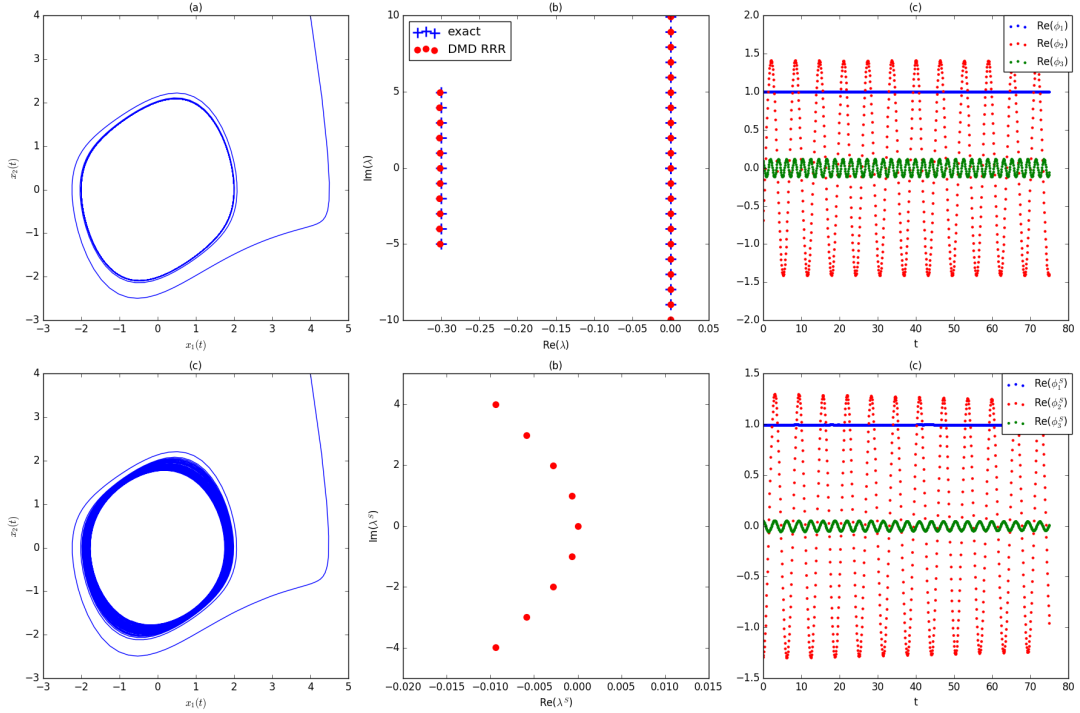


Figure 7: Van der Pol oscillator (86). Deterministic case: (a) solution; (b) Koopman eigenvalues; (c) the time evolution of real part of Koopman eigenfunctions. Stochastic case: (d) solution; (e) stochastic Koopman eigenvalues; (f) the time evolution real part of stochastic Koopman eigenfunctions. The threshold for the residuals is set to 0.001.

#### 4.3.4 Noisy Lotka-Volterra predator-prey system

Here we consider the Lotka-Volterra system with competition describing the predator prey system with two species. Such type of a model is typically used by biologists and ecologists for modeling the population dynamics. The corresponding noisy system is given

by:

$$\begin{aligned} dX_1 &= (a_1 - b_1X_2 - c_1X_1) X_1 dt + \sigma_1 X_1 dW_t^1 \\ dX_2 &= (-a_2 + b_2X_1 - c_2X_2) X_2 dt + \sigma_2 X_2 dW_t^2. \end{aligned} \quad (87)$$

The model parameters  $a_1, b_1, c_1, a_2, b_2, c_2 > 0$  depend on the particular species under consideration. The intensity of the noise is modeled by nonnegative parameters  $\sigma_1$  and  $\sigma_2$ .

We first consider the properties of the deterministic system. The first quadrant  $\mathbb{R}_+^2 = \{(X_1, X_2) | X_1 \geq 0, X_2 \geq 0\}$  is the domain of evolution of the system. There is an equilibrium point on the  $x_1$ -axis  $(\frac{a_1}{c_1}, 0)$ . If the nullclines  $a_1 - b_1X_2 - c_1X_1 = 0$  and  $-a_2 + b_2X_1 + c_2X_2 = 0$  do not intersect, then the equilibrium point on the positive  $x_1$  axis is unique. On the other hand, if these lines do intersect at the point  $(x_1^*, x_2^*)$  it can be shown that this is an asymptotically stable equilibrium point whose basin of attraction is  $\mathbb{R}_+^2$  with the exception of the axes. The considered system can be linearized around the equilibrium point. As known from Hartman-Grobman theorem, if all the eigenvalues of the Jacobian matrix at the fixed point have negative (or positive) real part, then there exist a  $\mathcal{C}^1$ -diffeomorphism  $\mathbf{h}$  defining the conjugacy map that locally transform the system to the linear one. Even more, as proved in [15], if all eigenvalues have negative real part (i.e. fixed point is exponentially stable) the  $\mathcal{C}^1$ -diffeomorphism  $\mathbf{h}$  is defined on the whole basin of attraction and the system is conjugate to the linear one globally on the basin of attraction. In the stochastic case, for small enough  $\sigma_1$  and  $\sigma_2$ , the introduced noise does not change the nature of the solution.

We select  $a_1 = 1.0$ ,  $b_1 = 0.5$ ,  $c_1 = 0.01$ ,  $a_2 = 0.75$ ,  $b_2 = 0.25$ ,  $c_2 = 0.01$ . The off-axes equilibrium point is equal to  $(x_1^*, x_2^*) = (3.07754, 1.93845)$ . Since the eigenvalues of the Jacobian matrix at this point are equal to  $\lambda_{1,2} = -0.02500799 \pm 0.863524i$ , we conclude that this is an exponentially stable fixed point and that the system is conjugate to the linear one in its basin of attraction.

To numerically evaluate the eigenvalues and eigenfunctions of the Koopman operator we use, as in the Van der Pol oscillator example, the Hankel DMD RRR algorithm, where the Hankel matrix is defined for the scalar observable function  $f(X_1, X_2) = X_1 + X_2$ . We use the matrix with  $n = 100$  rows and  $m = 250$  columns. By taking into account only the eigenvalues related to the eigenvectors with the residuals smaller than  $\varepsilon = 10^{-3}$ , several leading eigenvalues of the Koopman operator are captured with high accuracy (see Figure 8). The principle eigenvalues  $\lambda_{1,2}$  are calculated with the accuracy greater than  $10^{-6}$ .

In the stochastic case, the variance parameters are set to  $\sigma_1 = \sigma_2 = 0.05$ . The solution of the stochastic equation is evaluated as an average solution over  $N = 1000$  trajectories starting at the same initial point (see Figure 8). The principal eigenvalues of the Koopman operator in the considered stochastic case evaluated by using the larger Hankel matrix than in deterministic case, with  $n = 250$  and  $m = 750$ , have negative real part, which means that the exponentially stable fixed point exists, thus the nature of the solution is not changed.

By using Proposition 6, we expect that the principal eigenvalues of the stochastic Koopman operator do not change by introducing the multiplicative noise for which  $\sigma_1 = \sigma_2$ . In fact, it seems that the position of the expectation fixed point is the same as the position of the fixed point in the deterministic case.

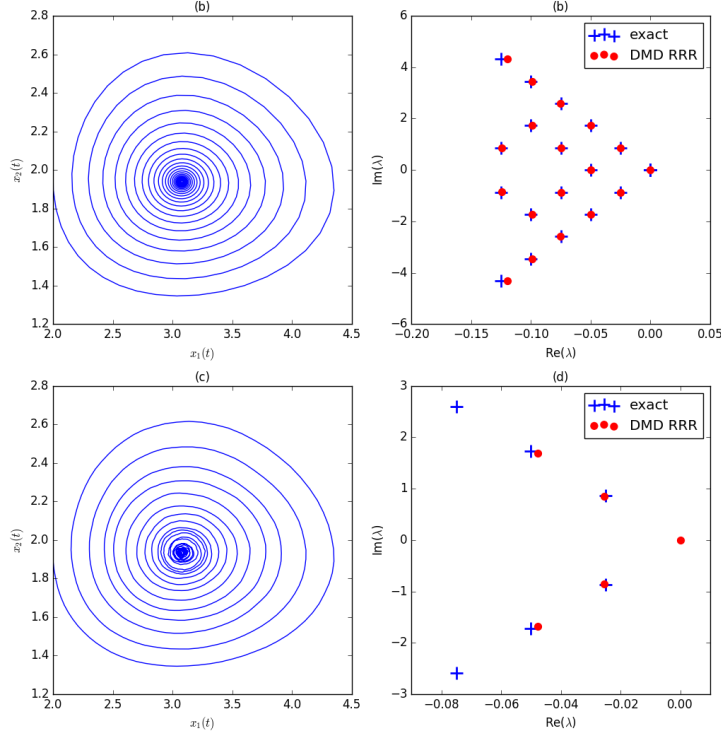


Figure 8: Lotka-Volterra system (87). Deterministic case: (a) solution; (b) Koopman eigenvalues. Stochastic case: (a) solution; (b) stochastic Koopman eigenvalues. The threshold for the residuals is set to 0.001.

## 5 Conclusion

In this work we provide a definition of the stochastic Koopman operator associated to the RDS. We explore the spectral decomposition of the stochastic Koopman operators related to the different type of RDS: discrete RDS, RDS driven by RDE and RDS driven by SDE. In the linear case, for all considered classes of RDS, we determine the so called principal eigenvalues and principal eigenfunctions of each operator family member. Under certain conditions, when the generator of the stochastic Koopman family exists, we derive its action on the observable functions and explore the properties of its eigenfunctions.

To numerically compute the eigenvalues and the eigenfunctions we use the new DMD RRR algorithm [5]. We also prove that under the assumption of ergodicity of RDS and the existence of finite dimensional invariant Krylov subspace, the eigenvalues computed by applying DMD RRR algorithm to the Hankel matrix converge to the true eigenvalues and eigenfunctions of the stochastic Koopman operator. The results presented in numerical examples show good performance of numerical algorithms applied to RDS for evaluation of the spectral objects of the stochastic Koopman operator.

Despite the fact that the most of the results for the eigenvalues and eigenfunctions are given for the linear case, the applicability of the results are much wider, since according to the stochastic version of Hartman-Grobman theorem [2], the RDS around the hyperbolic



fixed point can be at least locally transformed to the linear ones via  $\mathcal{C}^1$ -diffeomorphic conjugacy map.

## Acknowledgment

This research has been supported by the DARPA Contract HR0011-16-C-0116 "On A Data-Driven, Operator-Theoretic Framework for Space-Time Analysis of Process Dynamics" and AFOSR grants FA9550-08-1-0217 and FA9550-17-C-0012. We are thankful to Milan Korda and Allan Avila for useful comments.

## References

- [1] H. Arbabi and I. Mezić. Ergodic theory, Dynamic Mode Decomposition and Computation of Spectral Properties of the Koopman operator. *ArXiv e-prints*, November 2016.
- [2] L. Arnold. *Random Dynamical Systems*. Springer, 1998.
- [3] S. Bagheri. Koopman-mode decomposition of the cylinder wake. *J. Fluid Mech.*, 726:596–623, 2013.
- [4] M. Budišić, R. Mohr, and I. Mezić. Applied Koopmanism. *Chaos*, 22(4):596–623, 2012.
- [5] Z. Drmač, I. Mezić, and R. Mohr. On an enhanced dynamic mode decomposition. *arXiv preprint*, 2017.
- [6] P. Gaspard, G. Nicolis, A. Provata, and S. Tasaki. Spectral signature of the pitchfork bifurcation: Liouville equation approach. *Phys. Rev. E*, 51(1), 1995.
- [7] D. Giannakis. Data-driven spectral decomposition and forecasting of ergodic dynamical systems. *arXiv preprint arXiv: 1507.02338*, September 2016.
- [8] M. S. Hemati, C. W. Rowley, E. A. Deem, and L. N. Cattafesta. De-biasing the dynamic mode decomposition for applied koopman spectral analysis. *Theor. Comp. Fluid. Dyn.*, 31(4):349–368, 2017.
- [9] B. J. Hollingsworth. *Stochastic Differential Equations: A Dynamical Systems Approach*. Dissertation, Auburn University., 2008.
- [10] M. Hutzenthaler and A. Jentzen. Numerical approximations of stochastic differential equations with non-globally lipschitz continuous coefficients. *Mem. Amer. Math. Soc.*, 236(1112), 2015.
- [11] O. Junge, J. E. Marsden, and I. Mezić. Uncertainty in the dynamics of conservative maps. In *43rd IEEE Conference on Decision and Control*, 2004.
- [12] B.O. Koopman. Hamiltonian systems and transformation in Hilbert space. *P. Natl. Acad. Sci. USA*, 17(5):315, 1931.

- [13] M. Korda and I. Mezić. On Convergence of Extended Dynamic Mode Decomposition to the Koopman Operator. *ArXiv e-prints*, March 2017.
- [14] J. N. Kutz, X. Fu, and S. L. Brunton. Multiresolution dynamic mode decomposition. *SIAM J. Appl. Dyn. Syst.*, 15(2):713–735, 2016.
- [15] Y. Lan and I. Mezić. Linearization in the large of nonlinear systems and koopman operator spectrum. *Physica D*, 242(1):42–53, 2013.
- [16] S. Maćešić, N. Črnjarić Žic, and I. Mezić. Koopman operator family spectrum for nonautonomous systems - part i. *arXiv preprint arXiv:*, March 2017.
- [17] I. Mezić. Spectral properties of dynamical systems, model reduction and decompositions. *Nonlinear Dynam.*, 41(1):309–325, 2005.
- [18] I. Mezić. Analysis of fluid flows via spectral properties of the Koopman operator. *Annu. Rev. Fluid Mech.*, 45:357–378, 2013.
- [19] I. Mezić. Koopman Operator Spectrum and Data Analysis. *ArXiv e-prints*, February 2017.
- [20] I. Mezić and Surana A. Koopman mode decomposition for periodic/quasi-periodic time dependence. *IFAC-PapersOnLine*, 49(18):690 – 697, 2016. 10th IFAC Symposium on Nonlinear Control Systems NOLCOS 2016.
- [21] I. Mezić and A. Banaszuk. Comparison of systems with complex behavior. *Physica D*, 197(1):101–133, 2004.
- [22] J.L. Proctor and P. A. Eckhoff. Discovering dynamic patterns from infectious disease data using dynamic mode decomposition. *Int. Health*, 7:139–145, 2015.
- [23] A. Rößler. Runge–kutta methods for the strong approximation of solutions of stochastic differential equations. *SIAM J. Numer. Anal.*, 48(3):922–952, 2010.
- [24] C.W. Rowley, I. Mezić, S. Bagheri, P. Schlatter, and D.S. Henningson. Spectral analysis of nonlinear flows. *J. Fluid Mech.*, 641(1):115–127, 2009.
- [25] P.J. Schmid. Dynamic mode decomposition of numerical and experimental data. In *Sixty-First Annual Meeting of the APS Division of Fluid Dynamics*, 2008.
- [26] P.J. Schmid. Dynamic mode decomposition of numerical and experimental data. *J. Fluid Mech.*, 656(1):5–28, 2010.
- [27] P.J. Schmid, L. Li, M.P. Juniper, and O. Pust. Applications of the dynamic mode decomposition. *Theor. Comp. Fluid Dyn.*, 25(1):249–259, 2011.
- [28] A. S. Sharma, I. Mezić, and B. J. McKeon. Correspondence between koopman mode decomposition, resolvent mode decomposition, and invariant solutions of the navier-stokes equations. *Phys. Rev. Fluids*, 1(3):032402, 2016.
- [29] T. Shnitzer, R. Talmon, and J.J Slotine. Manifold learning with contracting observers for data-driven time-series analysis. *IEEE T. Signal Proces.*, 65:904–918, 2017.

- [30] J.L. Strand. Random ordinary differential equations. *J. Diff. Equations*, 7:538–553, 1970.
- [31] Y. Susuki and I. Mezić. Nonlinear Koopman modes and a precursor to power system swing instabilities. *IEEE T. Power Syst.*, 27(3):1182–1191, 2012.
- [32] Y. Susuki and I. Mezić. A prony approximation of koopman mode decomposition. In *Decision and Control (CDC), 2015 IEEE 54th Annual Conference on Decision and Control*, 2015.
- [33] Y. Susuki, I. Mezić, F. Raak, and Hikiyara T. Applied koopman operator theory for power system technology. *Nonlinear Theory and Its Applications, IEICE*, 7(4):430–459, 2016.
- [34] N. Takeishi, Y. Kawahara, and T. Yairi. Subspace dynamic mode decomposition for stochastic Koopman analysis. *Phys. Rev. E*, 96:033310, 2017.
- [35] A. Tantet, M. D. Chekroun, H. A. Dijkstra, and J. D. Neelin. Mixing Spectrum in Reduced Phase Spaces of Stochastic Differential Equations. Part II: Stochastic Hopf Bifurcation. *ArXiv e-prints*, May 2017.
- [36] J. H. Tu, C. W. Rowley, D. M. Luchtenburg, S. L. Brunton, and J. N. Kutz. On dynamic mode decomposition: theory and applications. *J. Comp. Dyn.*, 1(2):391–421, 2014.
- [37] M.O. Williams, I.G. Kevrekidis, and C.W. Rowley. A data-driven approximation of the Koopman operator: extending dynamic mode decomposition. *J. Nonlinear Sci.*, (25):1307–1346, 2015.